BANG-BANG EXCITATION CONTROL OF POWER SYSTEM STABILITY

A Thesis

Presented to

the Faculty of Graduate Studies and Research

University of Manitoba

In Partial Fulfillment

of the Requirements for the Degree

Master of Science in Electrical Engineering

---

by

Gordon W. Ryckman

May 1970

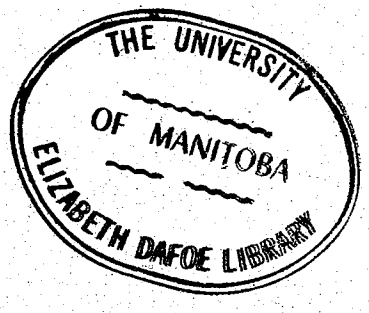

ABSTRACT

This thesis represents a study of the use of "bang-bang" excitation control to improve the stability of a synchronous generator connected to an infinite bus. A third order model of the system is used with the constants of the model determined from measurements on an actual machine. This model is used as the basis of an analog computer simulation. The system stabilizing requirements are established and it is shown that a signal proportional to accelerating power provides an adequate increase in the stability of the system. It is also shown that an equivalent bang-bang signal produces an even greater increase in stability.

ACKNOWLEDGEMENT

The author wishes to acknowledge his indebtedness to Professor G. W. Swift for his guidance and assistance and to Professor R. W. Menzies for his helpful discussions on the subject.

The financial assistance from the National Research Council through a Postgraduate Scholarship and under grant number A2780 is also acknowledged.

TABLE OF CONTENTS

LIST OF TABLES

LIST OF ILLUSTRATIONS

FIGURE

FIGURE PAGE

I. INTRODUCTION

The problem of synchronous machine stability and power system damping has received much attention in the past. A great deal of important research has been done yielding many significant improvements. It has been indicated that there are four basic methods of improving power system damping[15*]. These include: load or dynamic braking, posicast switching (of capacitors), machine (excitation) voltage control, and locally controlled capacitor switching. The use of excitation control has proven to be the most useful of the above methods and consequently has received the greatest amount of attention. Improvements in this regard include: the use of continuously-acting regulators[4], the introduction of solid state exciters[2], and more recently, the use of linear feedback theory and the application of additional stabilizing signals (usually proportional to speed error)[20] to improve system damping. Optimal control theory[22, 27] and sampled data control theory[19] have also been successfully applied to the problem.

Intuitive reasoning leads one to the conclusion that a bang-bang or maximum effort control could be more effective than a conventional proportional controller in damping synchronous machine oscillations. This intuitive reasoning is further supported by the fact that the solution to most time optimal control problems is bang-bang in nature[1].

---

* Numeral superscripts refer to Bibliography.

The design of a bang-bang control system could be based on one of the following:

1) Time optimal control theory[1, 22]

2) Posicast and negicast control theory[16, 21, 11]

to yield a deadbeat solution, or

3) A study of the special stabilizing requirements of synchronous machines.

Bang-bang stabilizing signals have been successfully applied to improve synchronous machine stability. In a paper by O. J. M. Smith[22], a solution which is essentially time optimal is presented. The main disadvantage of such a solution is the difficulty in applying it to an actual machine. As with any optimal solution, all available information concerning the state of the system must be obtained. G. A. Jones[11], on the other hand, has contributed a solution which is almost deadbeat in nature. This type of stabilization is easily applied to an actual machine but lacks generality in that it is applicable to only one very special type of disturbance. "Good" stabilization should be capable of providing adequate damping over a wide spectrum of possibilities.

This thesis describes the research undertaken to ascertain the stabilizing requirement of a synchronous generator and to develop a simple bang-bang stabilizing control which would provide greater damping than an "equivalent" proportional control for a wide spectrum of possibilities.

The system considered in this study consists of a four kilovolt amperes wye-connected synchronous generator

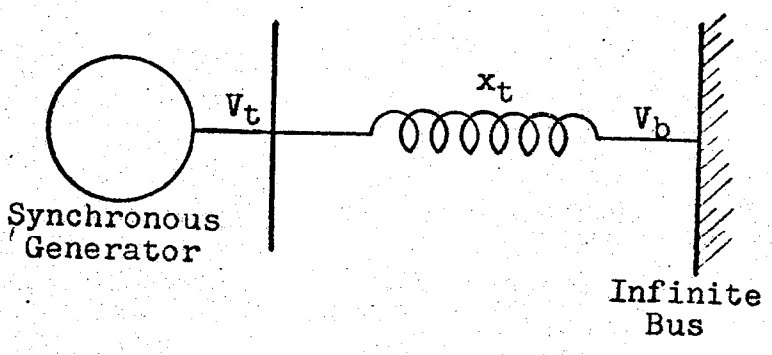

Figure 1. Single Line Diagram of the System

attached to an infinite bus through external reactance and driven by a d.c. shunt-connected motor. A single line representation of the system is shown in Figure 1.

It is established that the basic stabilizing requirement of this system, as with most synchronous machines, is a need for increased system damping. This implies the use of a stabilizing signal proportional to speed deviations. A considerable amount of phase lag is introduced into the stabilizing loop by the field and exciter time constants. It is shown that this lag can be adequately compensated for by use of a signal proportional to accelerating power. This effectively adds approximately eighty degrees of phase lead to the stabilizing signal. To increase the effectiveness of the stabilization, a bang-bang signal is introduced. This signal is such that it is in phase with the accelerating power and has a magnitude of plus or minus the ceiling voltage of the exciter. It is shown that this signal does provide better stabilization than the more conventional proportional signal. Due to the nature of the signal, it is relatively easy to apply to an actual machine, and does provide adequate stabilization for a wide spectrum of possibilities.

II. MODELLING THE SYSTEM

The Heffron and Phillips Model

The Heffron and Phillips model[10] is used as the basis for a stability study of the system shown in Figure 1. This model represents a synchronous generator connected to an infinite bus as a third order system linearized about a particular operating point. A block diagram of the model is given in Figure 2, and a phasor diagram of the system is shown in Figure 3.

The constants K_1 - K_6 are the Heffron and Phillips constants and may be calculated from the following expressions*:

$$K_1 = (V_{qo}V_b\cos\delta_o)/(x_q + x_t) + (V_{tdo}V_b\sin\delta_o)\,(1 - x_d'/x_q)/(x_d' + x_t) \quad (2.1)$$

$$K_2 = (V_b\sin\delta_o)/(x_d' + x_t) \quad (2.2)$$

$$K_3 = (x_d' + x_t)/(x_d + x_t) \quad (2.3)$$

$$K_4 = (x_d - x_d')\,(V_b\sin\delta_o)/(x_d + x_t) \quad (2.4)$$

$$K_5 = (V_{tdo}/V_{to})\,(x_qV_b\cos\delta_o)/(x_q + x_t) - (V_{tqo}/V_{to})\,(x_d'V_b\sin\delta_o)/(x_d' + x_t) \quad (2.5)$$

$$K_6 = (V_{tqo}/V_{to})x_t/(x_d' + x_t) \quad (2.6)$$

Nonlinearities and losses in the system are considered to the extent that the six constants are evaluated

---

* Zero subscripts indicate that the parameter is evaluated at an operating point.

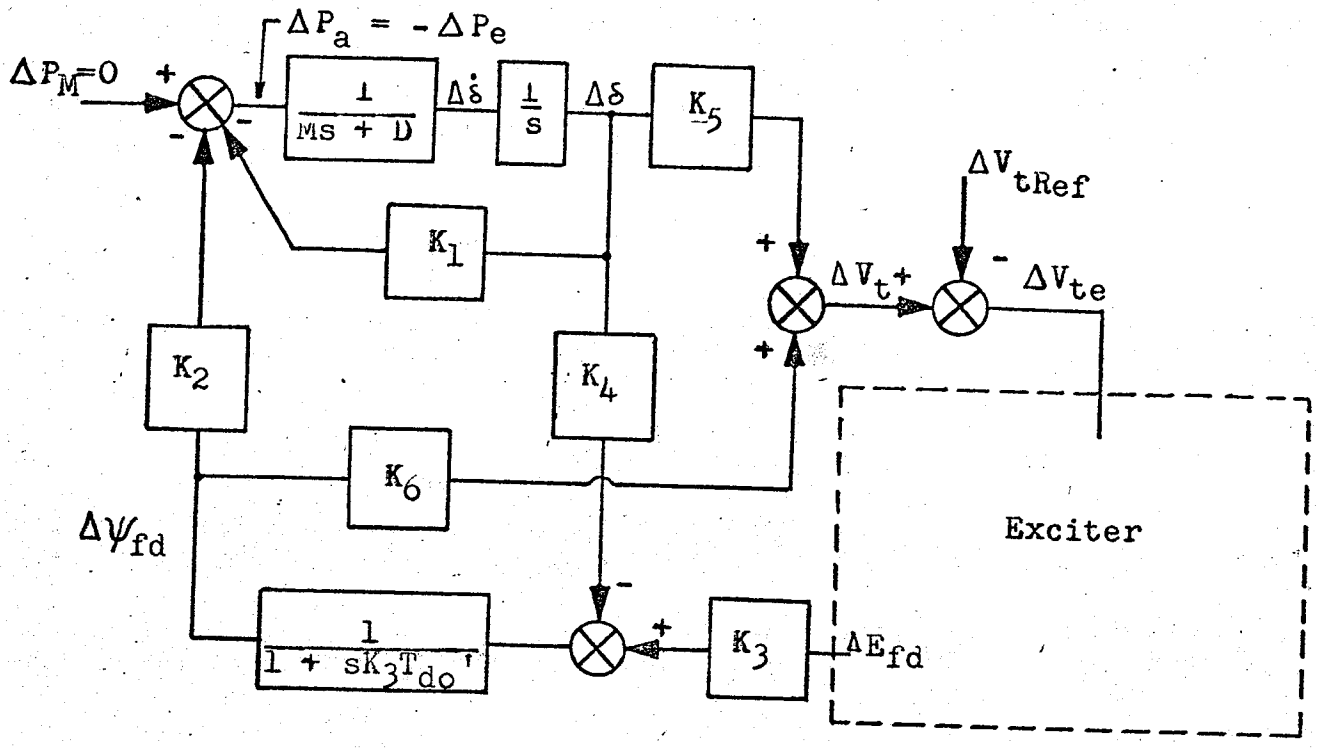

Figure 2. The Heffron and Phillips Model

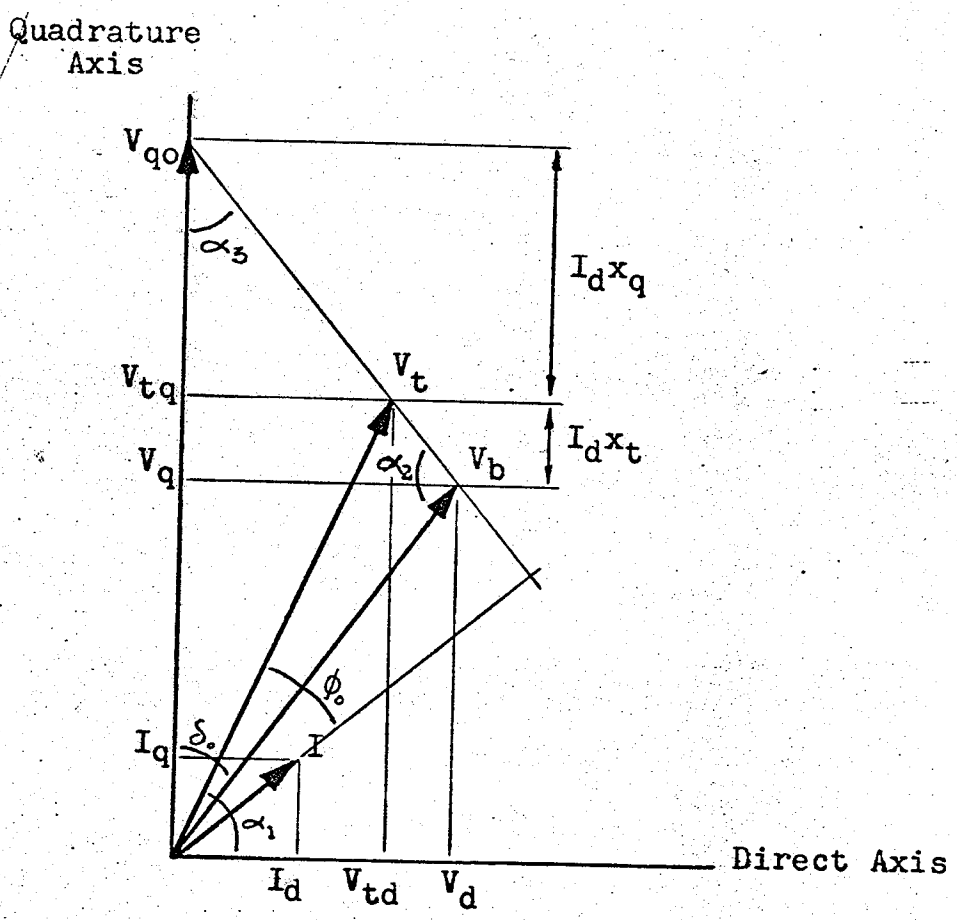

Figure 3. Phasor Diagram for a Synchronous Generator Connected to an Infinite Bus

for several different operating points using data obtained from measurements on an actual machine.

The following is a list of assumptions inherent in the use of the Heffron and Phillips model:

1) The effects of amortisseur windings are neglected.

2) Voltages due to rate of change of direct and quadrature axis flux linkages and to change of speed are not considered.

3) Armature and transmission line resistances are not included.

4) Harmonics are neglected.

It is also important to realize that the Heffron and Phillips model is essentially a single-phase equivalent. The analysis, therefore, assumes symmetrical conditions at all times.

Measurement of System Parameters

In order to evaluate the six Heffron and Phillips constants, values for x_d, x_q, x_d' and x_t must be found. Values for T_{do}', M and D must also be determined to complete the Heffron and Phillips model

A Note on the Per Unit System

The Heffron and Phillips model is derived from the basic synchronous machine equations developed by R. H. Park[17]. Consequently, the parameters of this model are given in the same non-reciprocal per unit system as Park used in his original paper. As in an ordinary reciprocal system, all per unit values are based on the per phase values of rated stator voltage and current. This yields

the following base quantities:

1) Base voltage = 120 volts

2) Base current = 10.5 amperes

3) Base volt amperes = 1.26 kilovolt amperes

4) Base impedance = 11.4 ohms

In this non-reciprocal system, however, ψ_d, ψ_{fd}, I_{fd} and E_{fd} are all unity for open circuit normal voltage on the air-gap line[18].

Measurement of Direct Axis Synchronous Reactance, x_d

A slip test will yield values for both x_d and x_q. In this test, however, the "slipping" causes induced currents, especially in the damper windings. This may cause very serious errors especially in small machines. Most authors[26, 9] agree that a combination of an open circuit voltage test and a short circuit current test will give a much more accurate value for x_d.

In the open circuit voltage test, the machine is run at synchronous speed and a graph of open circuit phase voltage versus field current is made. To perform the short circuit current test, a three-phase short circuit is applied to the machine and line current is plotted against field current with the machine running at synchronous speed. Figure 4 shows the results of these tests. Using equation

$$x_d(\text{sat.}) = (E_{oc}/I_{sc})\Big|_{i_f = I_{fb}} \qquad (2.7)$$

(2.7) a value of 9.11 ohm or 0.797 per unit is established for x_d.

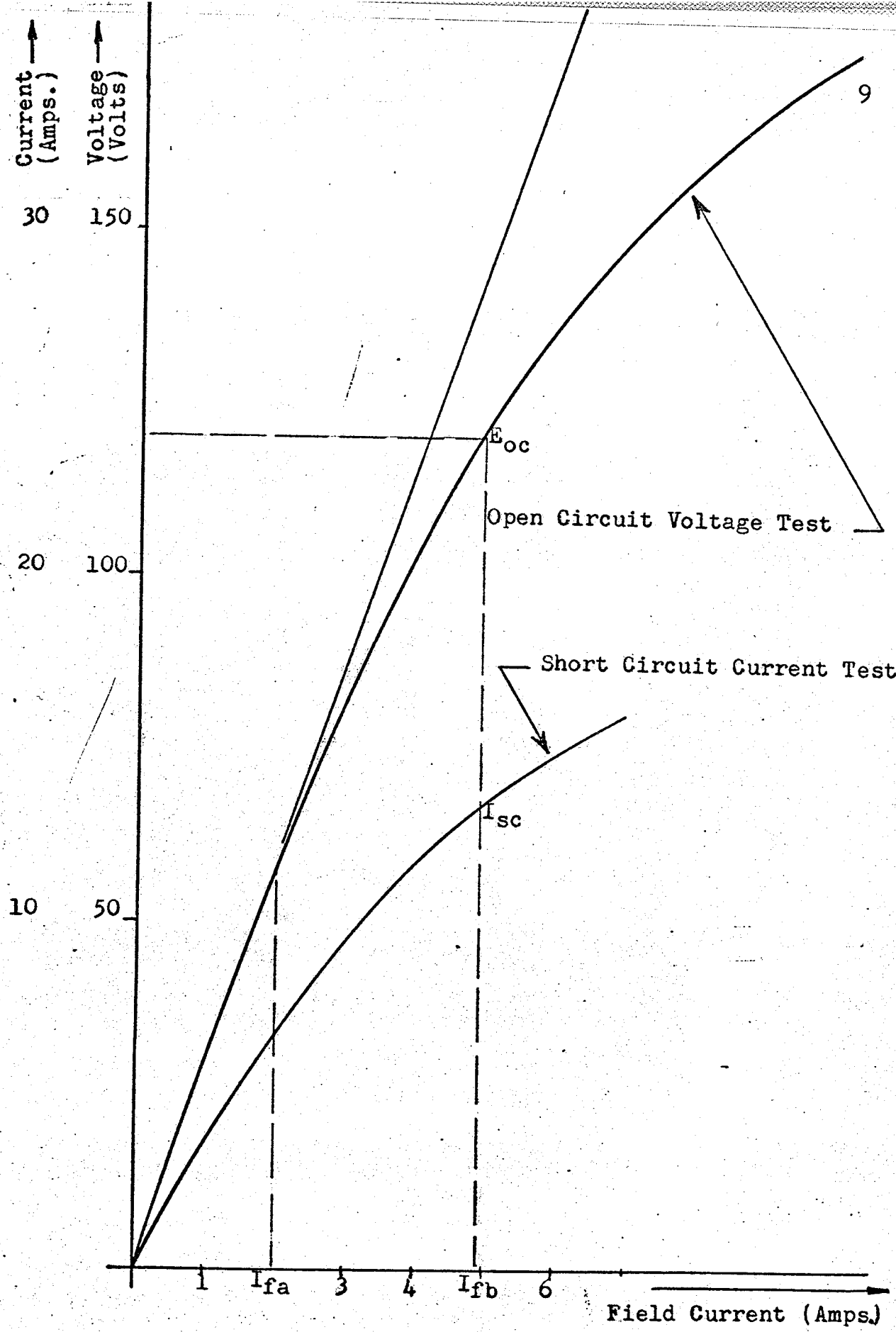

Figure 4. Open Circuit Voltage and Short Circuit Current Test Results

Measurement of Quadrature Axis Synchronous Reactance x_q

As mentioned in the previous section, x_q could be calculated directly from the slip test. A value of x_q could also be obtained indirectly from the slip test by finding the ratio of x_q to x_d and multiplying this value by the previously determined value of x_d. If the slip test is to be used, the indirect method is preferred since the effect of induced currents (as mentioned in the previous section) will be considerably reduced. There are, however, other disadvantages inherent in the slip test. The test is usually performed using very low values of stator voltage and an open field circuit. This means the machine is not operating under normal conditions and effects such as saturation will not be included. Error is also introduced in the interpretation of the resulting oscillograph.

The maximum lagging current test[9] eliminates these difficulties. In this test the machine is driven as an unloaded synchronous motor with rated stator voltage. With the field applied the machine will be synchronized with the line. When the field is removed synchronism will be maintained but as the field is reversed, the machine will slowly slip a pole. The ratio of stator voltage to maximum lagging current, measured just before the pole slips, yields a value for x_q. For the machine under test x_q was found to be 7.25 ohms or 0.634 per unit.

Measurement of Direct Axis Transient Reactance x'_d

Traditionally, x'_d is determined from a short circuit transient test. This test was performed but the results were not satisfactory. This is attributed to the following:

1) Very short time constants caused by the high resistance to inductance ratio characteristic of small machines.

2) A large second harmonic term which is usually negligible in larger machines, and

3) Difficulty in interpreting the oscillograph.

An indirect method is also available for the determination of x'_d. It has been shown[26] that x'_d bears the following relationship with x_d:

$$x'_d = (T_d'/T_{do}') \, x_d \qquad (2.8)$$

It has also been found that saturation causes a reduction in the value of x'_d given by equation (2.8). This reduction could be accounted for in one of two ways[26]: first, by a factor equal to the ratio of (field amperes at rated voltage on the air gap line) to (field amperes at rated voltage no load) - which equals 0.87 for the machine under test; second, by an empirical factor equal to 0.88. Equation (2.9) was, therefore, used to determine x'_d.

$$x'_d = .88 \, (T_d'/T_{do}') \, x_d \qquad (2.9)$$

Figure 5 illustrates the method used to determine the open circuit time constant. The machine is run at synchronous speed with the field supply adjusted to give rated open circuit stator voltage. Switch "S" is closed

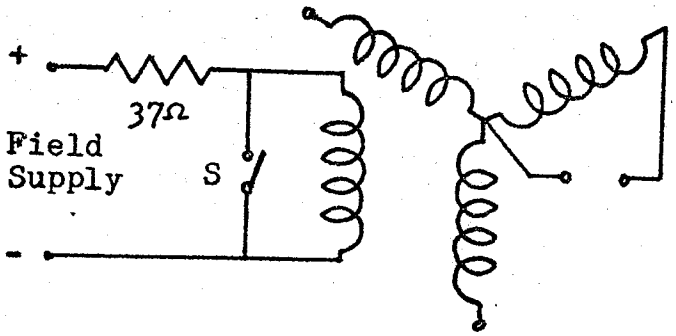

Figure 5. Measurement of T_{do}'

and an oscillograph of the terminal voltage decay is recorded. See Figure 6(a). The short circuit time constant is determined in the same way except a sustained short circuit is applied to the machine and an oscillograph of line current is recorded. This is shown in Figure 6(b). Figure 6 yields values of 0.120 seconds and 0.083 seconds for T_{do}' and T_{d}' respectively. Substituting these values in equation (2.9) gives a value of 5.50 ohms or 0.484 per unit for x'_d.

Measurement of External Reactance, x_t

A three-phase variac with neutral connections removed was used as a variable three-phase balanced inductance[25]. A plot of reactance versus variac setting is shown in Figure 7. Resistance of the variac was found to be approximately 10% of the reactance and was, therefore, neglected. The two most common values of reactance used are 0.048 per unit at 80% and 0.200 per unit at 71.5%.

Measurement of the Per-Unit Inertia Constant M and the Per Unit Prime Mover Damping, D

If a step input is applied to the field of a synchronous generator connected to an infinite bus, the electrical power will exhibit damped oscillations very similar to those characteristic of a second order under damped differential equation. There will also be a slight

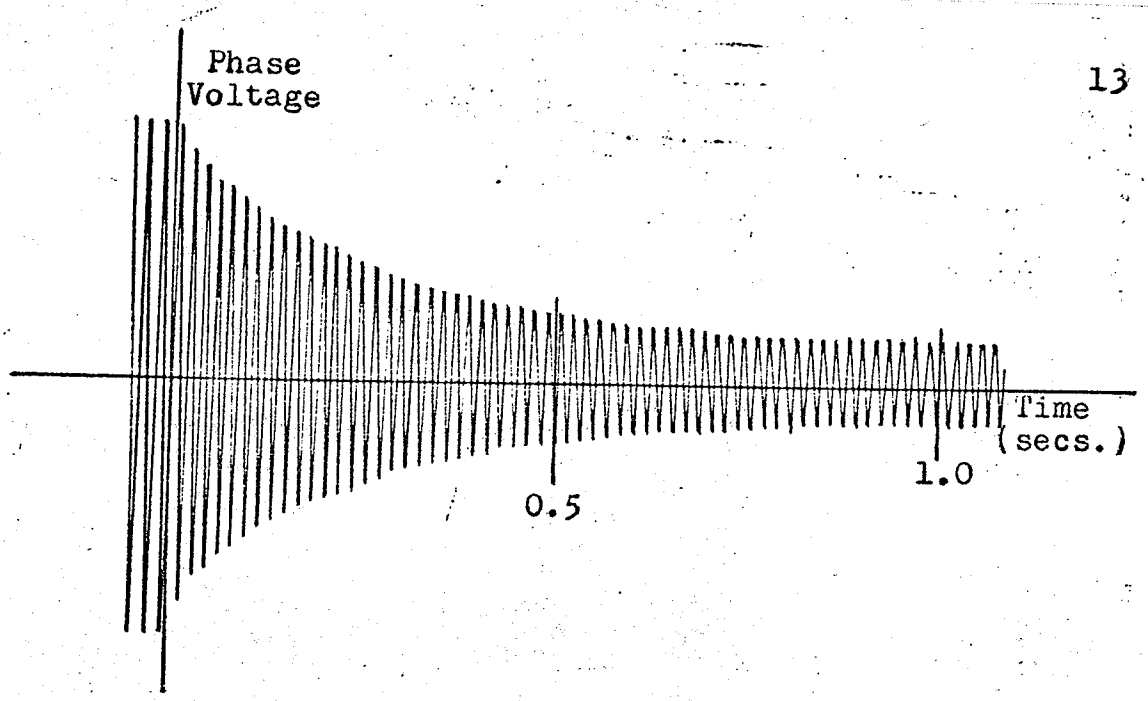

Figure 6a. Open Circuit Field-Decrement Test

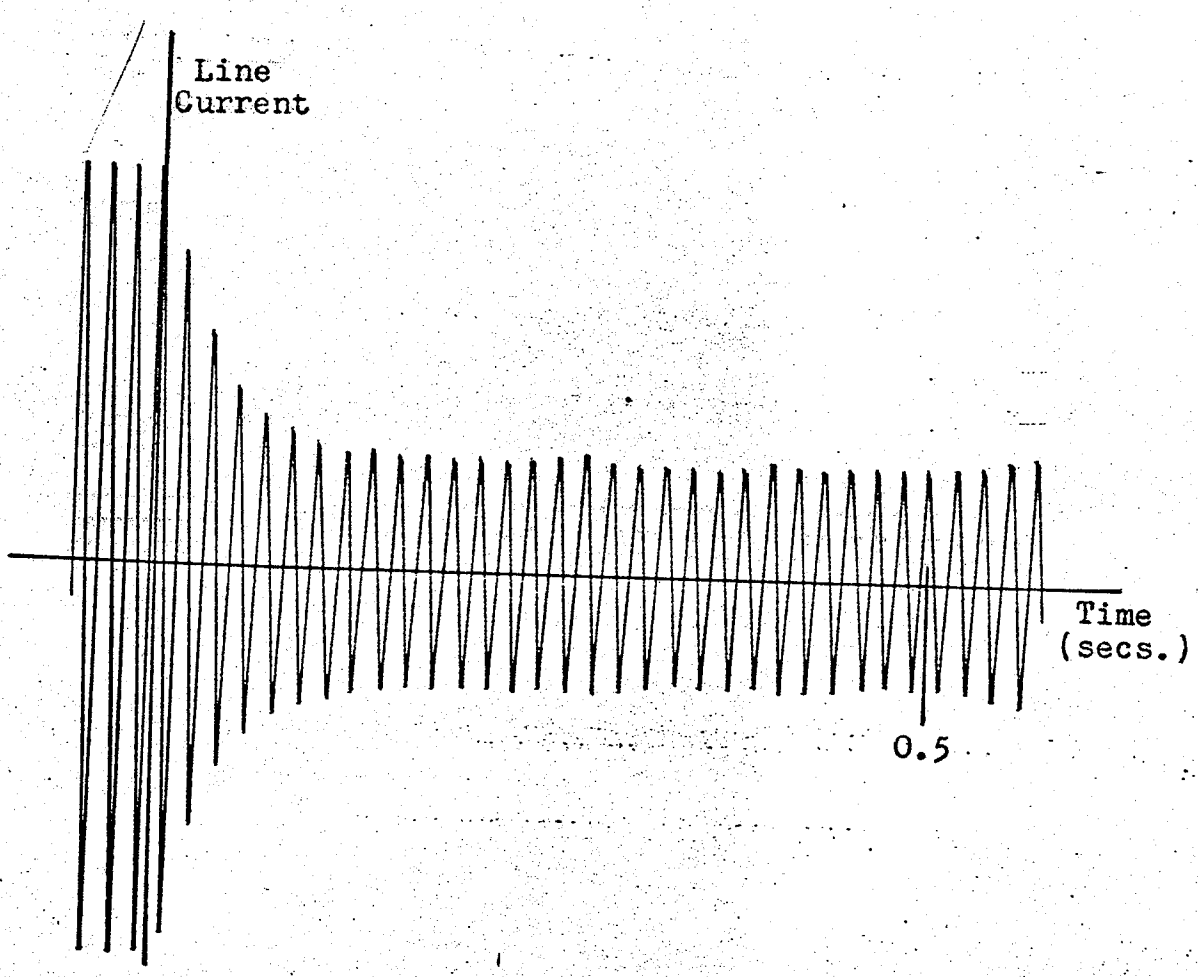

Figure 6b. Short Circuit Field-Decrement Test

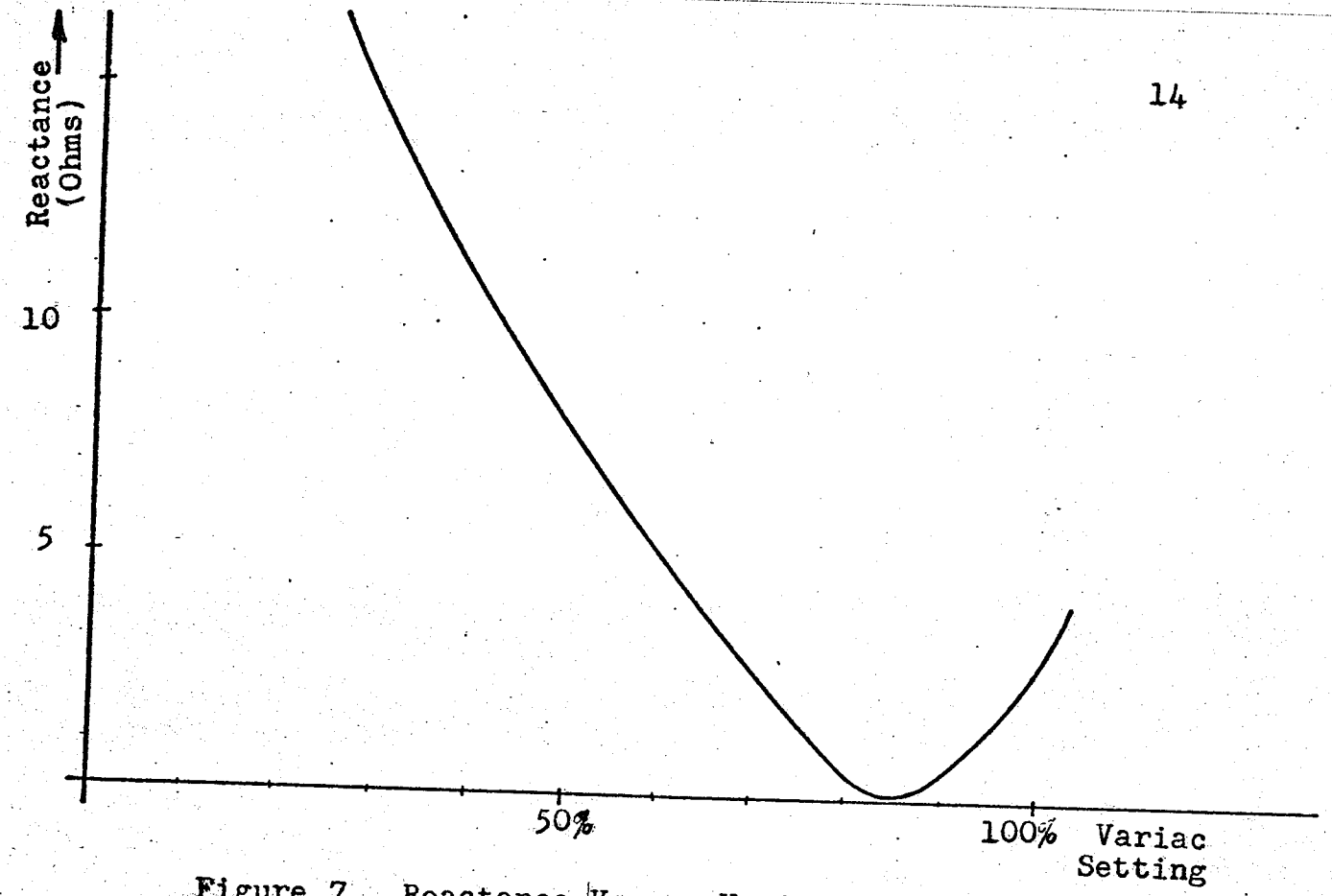

Figure 7. Reactance Versus Variac Setting

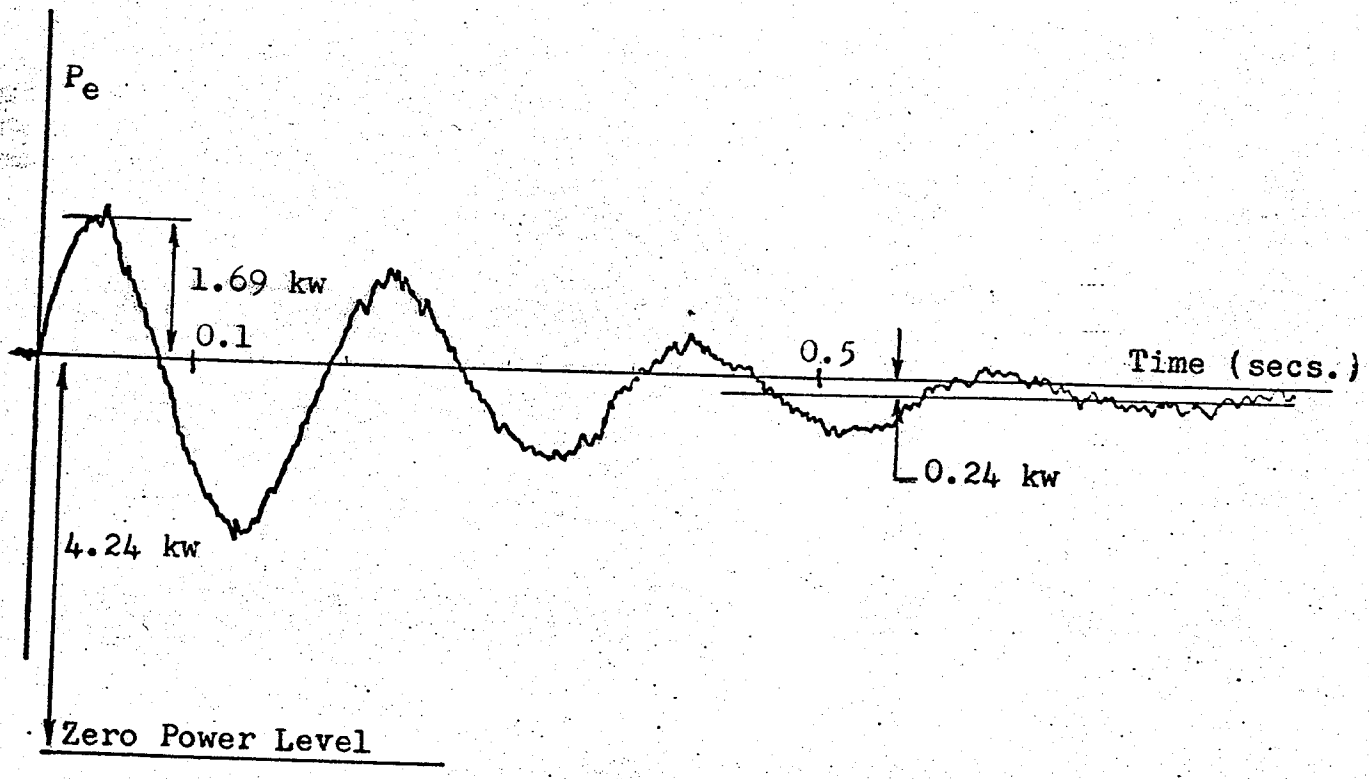

Figure 8. Variation in Electrical Power for a Step Change in Field Voltage

decaying negative bias term caused by the field time constant and a small positive or negative error caused by a change in the efficiency of the machine.

To measure M and D, the synchronous machine was connected to an infinite bus through an external impedance of 0.048 per unit. The system was adjusted to supply rated power at unity power factor. A step equal to 1.0 per unit was applied to the field. The resulting oscillations in electrical power are shown in Figure 8. The method used to obtain these oscillations is presented in Appendix A.

Neglecting the effect of armature reaction, machine losses, and field time constant, the synchronous generator may be represented by the second order system given in Figure 9. The transfer function of this system is given in equation (2.10).

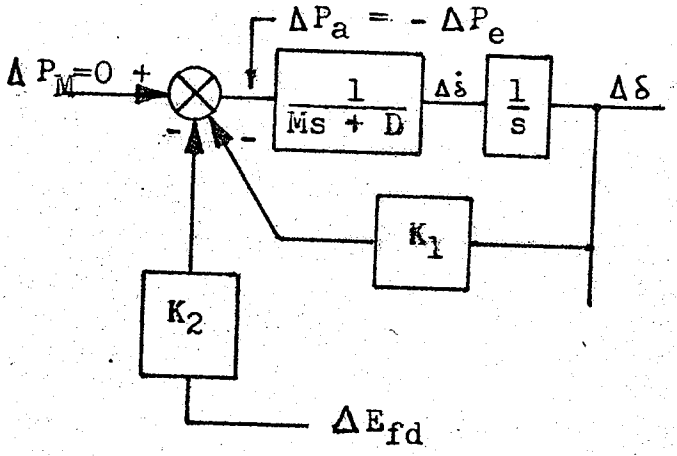

Figure 9. A Second Order Representation of the System

$$\Delta\delta(s)/\Delta E_{fd}(s) = (K_2/K_1)\left[(-K_1/M)/(s^2 + (D/M)s + (K_1/M))\right] \quad (2.10)$$

For a 1.0 per unit step in ΔE_{fd} we obtain

$$\Delta\delta(s) = (K_2/K_1)\left[(-K_1/M)/s(s^2 + (D/M)s + (K_1/M))\right] \quad (2.11)$$

Compare this expression with

$$C(s) = -w_n^2/s(s^2 + 2\zeta w_n s + w_n^2) \quad (2.12)$$

which has a time domain equivalent[8] of

$$C_{(t)} = (1/\beta)e^{-\zeta w_n t} \sin(w_n \beta t + \theta) - 1 \qquad (2.13)$$

with

$$\beta = \sqrt{1 - \zeta^2} \qquad (2.14)$$

and

$$\theta = \tan^{-1}(\beta/\zeta) \qquad (2.15)$$

Equations (2.11) and (2.12) are equal except for a constant factor of (K_2/K_1) provided the following two equations are satisfied:

$$(D/M) = 2\zeta w_n \qquad (2.16)$$

$$(K_1/M) = w_n^2 \qquad (2.17)$$

Hence, $\Delta\delta_{(t)}$ is of the same form as $C_{(t)}$. From Figure 9, $\Delta P_{e(t)}$ is given by

$$\Delta P_{e(t)} = K_1 \Delta\delta_{(t)} + K_2 \qquad (2.18)$$

The complete time domain expression for $\Delta P_{e(t)}$ is, therefore, given by equation (2.19).

$$\Delta P_{e(t)} = (K_2/\beta)e^{-\zeta w_n t} \sin(w_n \beta t + \theta) \qquad (2.19)$$

where β, w_n, ζ and θ are defined by equations (2.14) - (2.17). Measurements on Figure 8 yield values of 3.46 and 31.4 for (ζw_n) and (βw_n) respectively. At the given operating point K_1 is calculated to be 1.63.* The above information yields values of 0.00165 and 0.0114 for M and D respectively.

A summary of all necessary constant system parameters is given in Table 1.

---

*The evaluation of all six Heffron and Phillips constants for this and other operating points is discussed in the next section.

Measurement of Variable System Parameters V_b, V_{to} and δ_o

Evaluation of the six Heffron and Phillips constants requires a knowledge of V_b, V_{to}, and δ_o at the desired operating point. These quantities are determined for six different operating conditions by direct measurement using a voltmeter and stroboscope. The results are given in Table 2.

Evaluation of the Heffron and Phillips Constants

Additional relations for V_{tdo}, V_{tqo} and V_{qo} are established from the geometry of Figure 3. These are given in equations (2.20), (2.21) and (2.22) respectively.

$$V_{tdo} = (x_q V_b \sin\delta_o)/(x_q + x_t) \tag{2.20}$$

$$V_{tqo} = V_{to}\sin\alpha_1 \tag{2.21}$$

$$V_{qo} = (V_b \sin\alpha_2)/\sin\alpha_3 \tag{2.22}$$

Values for α_1, α_2 and α_3 may be found from the following:

$$\alpha_1 = \cos^{-1}\left[(V_b x_q \sin\delta_o)/V_{to}(x_q + x_t)\right] \tag{2.23}$$

$$\alpha_2 = \pi - (\delta_o + \alpha_1 - \phi_o) \tag{2.24}$$

$$\alpha_3 = \alpha_1 - \phi_o \tag{2.25}$$

Numerical values for K_1 - K_6 are calculated by substituting the information given in Tables 1 and 2 into equations (2.1) - (2.6) and (2.20) - (2.25). These values are tabulated in Table 3.

Analog Computer Circuit and Model Verification

The block diagram in Figure 2 was used directly for analog simulation of the system. For convenience, the simulation is slowed down by a factor of ten. The complete

Table 1. Constant System Parameters

Rated Output = 4.00 kilovolt amperes

Rated Terminal Voltage = 120 volts

Rated Line Current = 10.5 amperes

x_d = 9.11 ohms or .800 p.u.

x_q = 7.25 ohms or .630 p.u.

x'_d = 5.81 ohms or .480 p.u.

T_d' = .0825 seconds

T_{do}' = .120 seconds

M = .00165 p.u.

D = .0114 p.u.

$$x_t = \begin{cases} .550 \text{ ohms or } .0480 \text{ p.u. with variac at } 80\% \\ 2.40 \text{ ohms or } .200 \text{ p.u. with variac at } 71.8\% \end{cases}$$

Table 2. Variable System Parameters

Power Factor	x_t(p.u.)	V_b(p.u.)	V_{to}(p.u.)	δo(Deg.)
unity	.048	1.04	1.06	20.3
0.8 Leading	.048	1.04	1.08	14.4
0.8 Lagging	.048	1.05	1.05	39.3
unity	.200	1.05	1.06	31.5
0.8 Leading	.200	1.05	1.18	18.0
0.8 Lagging	.200	1.05	0.98	57.0

Table 3. Heffron and Phillips Constants
For Various Operating Points

p.f.	x_t(p.u.)	δ_o(Deg)	K_1	K_2	K_3	K_4	K_5	K_6
unity	.0480	20.3	1.63	.681	.623	.136	-.0244	.0863
0.8 Leading	.0480	14.4	1.36	.491	.623	.098	-.0210	.0886
0.8 Lagging	.0480	39.3	3.65	1.26	.623	.251	-.0446	.0735
unity	.200	31.5	1.30	.807	.680	.176	-.0892	.271
0.8 Leading	.200	18.0	1.06	.477	.680	.104	-.0650	.288
0.8 Lagging	.200	57.0	3.75	1.30	.680	.282	-.159	.215

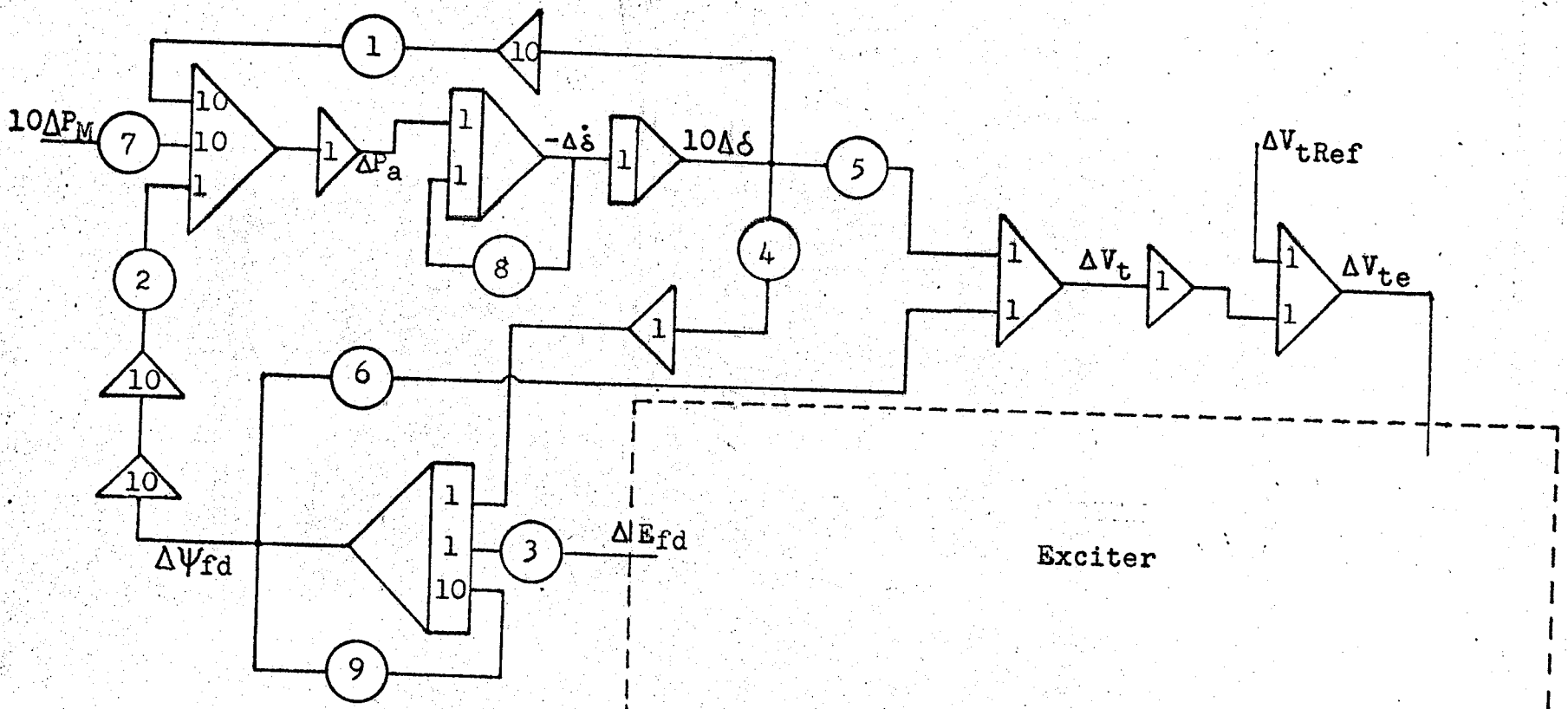

Pot Settings Given By:

#1 = .0605 K_1	#4 = .127 K_4	#7 = .605
#2 = .605 K_2	#5 = - .1 K_5	#8 = .690
#3 = 1.27 K_3	#6 = K_6	#9 = .127

Figure 10. Analog Computer Simulation of the System Including Time Scaling

analog computer representation, including time scaling is shown in Figure 10.

The Synchronous generator was adjusted to produce rated power at unity power factor. Figure 11 shows the variation in electrical power for a one per unit step change in field voltage. Figure 12 indicates the equivalent response of the simulated system. The most striking difference between the two plots is the 0.06 per unit steady state error in Figure 11. With the machine operating at unity power factor, maximum efficiency is attained. With a one per unit change in field voltage, the power factor becomes 0.65 leading and the efficiency decreases. A negative step in field voltage produces essentially the same effect since the efficiency decreases for lagging power factors as well. This effect is neglected in the Heffron and Phillips model. Furthermore, the response to a negative step in field voltage would be exactly opposite to that given in Figure 12. Figure 13 shows the response of the model to a one per unit step in ΔP_m. The results indicate a concave-up power versus torque angle curve. This is normal for many synchronous generators and was found to be the case for this particular machine. These curves also indicate the well-known fact[10] that operation with high external reactance or at a leading power factor causes the greatest problem as far as steady state stability is concerned.

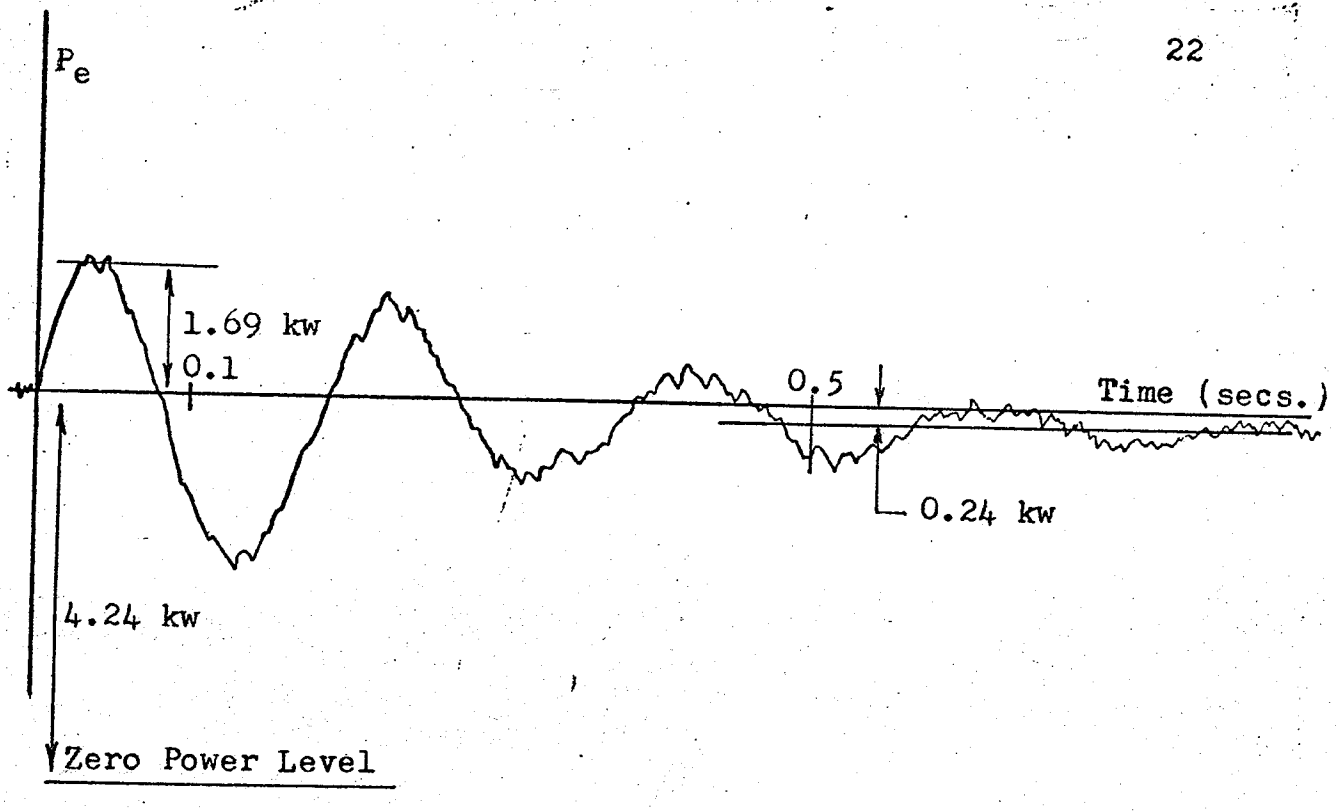

Figure 11. Variation in Electrical Power For a Step Change in Field Voltage Using the Actual Machine

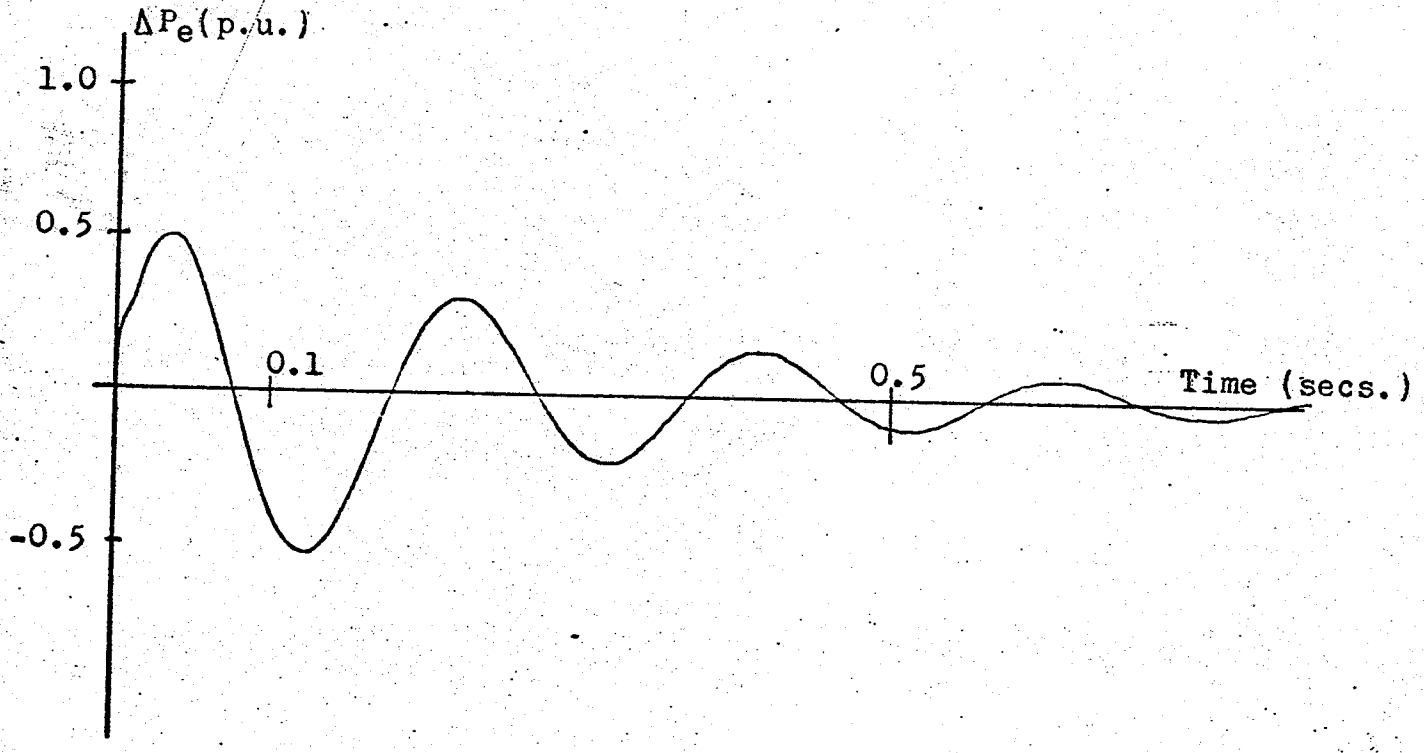

Figure 12. Variation in Electrical Power for a Step Change in Field Voltage Using the Simulated System

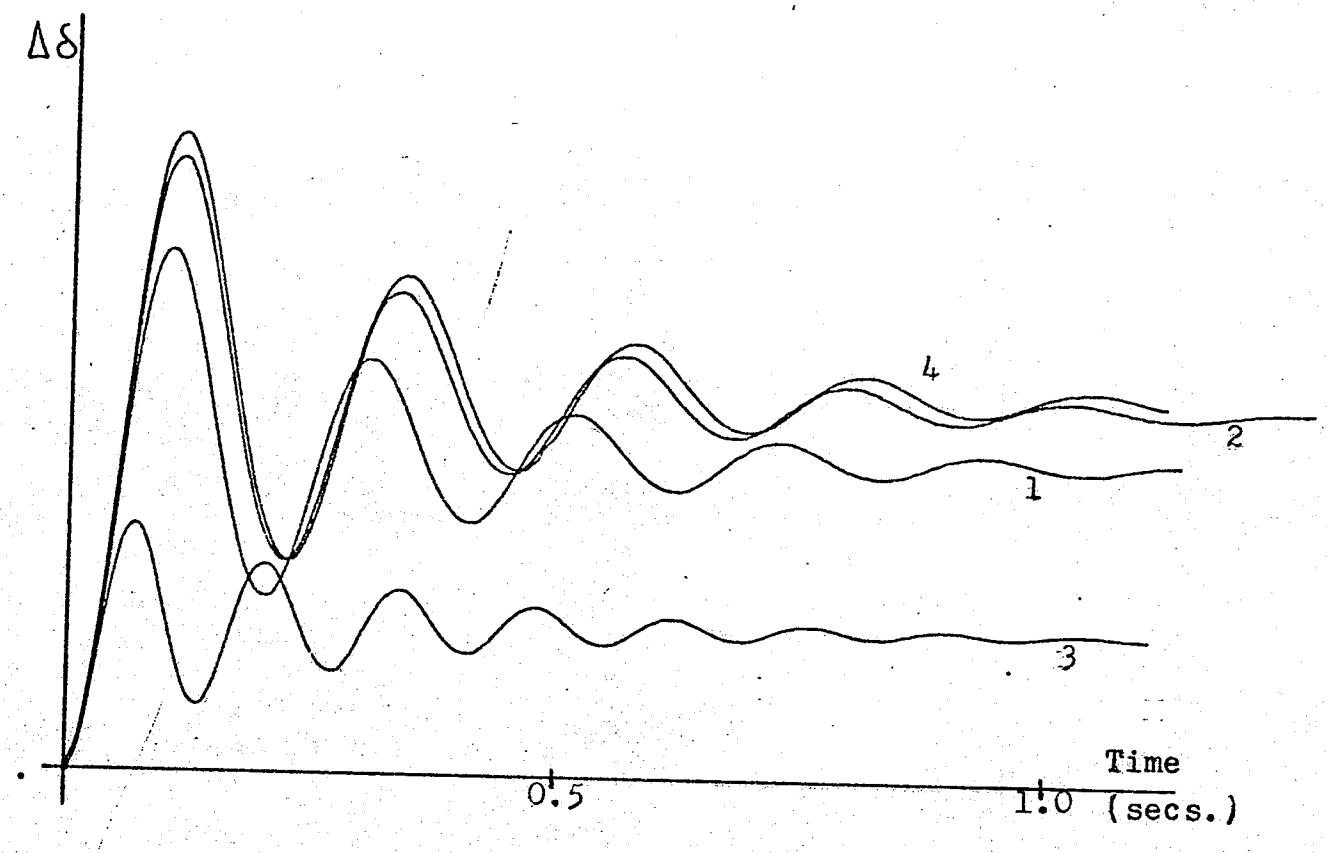

Figure 13. Deviation in $\Delta\delta$ For a Step Change in P_M with:

1) unity p.f. and x_t = .048 p.u.

2) 0.8 Leading p.f. and x_t = .048 p.u.

3) 0.8 Lagging p.f. and x_t = .048 p.u.

4) unity p.f. and x_t = .20 p.u.

III. VOLTAGE REGULATOR DESIGN

Before discussing the basic stablizing requirements of a synchronous generator, it is best to complete the block diagram of Figure 2 by adding voltage regulation through an appropriate transfer function representing the exciter. Figure 14 gives a block diagram of a simple exciter.

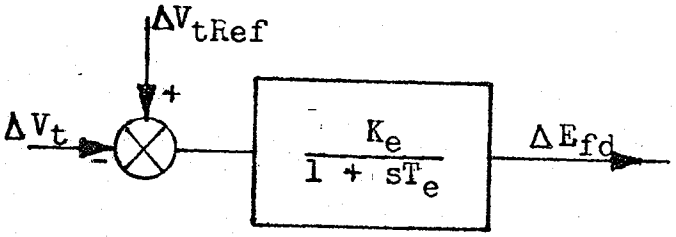

Figure 14. A Simple Exciter

If solid state excitation is to be used T_e may be chosen to equal 0.005 seconds. It will be shown that large values of K_e result in serious reductions in system damping. High values of K_e also produce underdamped oscillations in ΔV_t for a step command in $\Delta V_{t\ Ref}$. Low values of K_e result in a large steady state error in the desired terminal voltage. This undesirable situation may be remedied by including low frequency lag compensation.

One important criterion of voltage regulator performance is its operation under open circuit conditions for which case torque angle has no significance. With no load applied to the machine, K_3 and K_6 become unity and the corresponding voltage regulator loop is shown in Figure 15. For

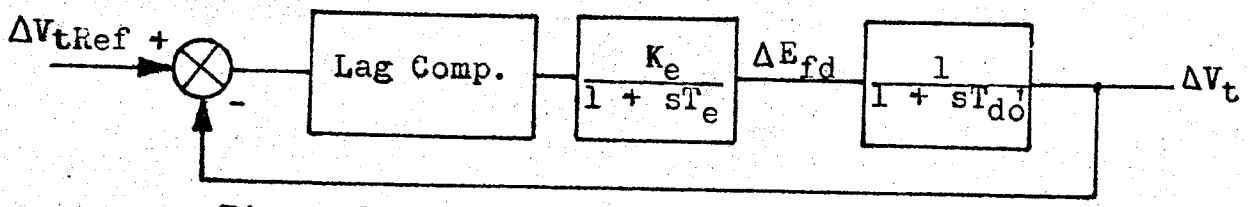

Figure 15. Voltage Regulator Loop Under Open Circuit Conditions

convenience the compensation is chosen to provide an additional gain of ten under steady state conditions. The "break-up point" of the compensation is chosen to coincide with the field break point ($1/T_{do}'$). With T_e equal to 0.005, the response of ΔV_t to a step charge is ΔV_t Ref. is shown in Figure 16 for several values of K_e. The effect of the lag compensation is also indicated. Choosing K_e equal to five, the complete exciter transfer function is shown in Figure 16. The corresponding Bode plot is shown in Figure 17. The broken lines indicate the Bode plot for the field and the complete Bode plot for the voltage regulator loop under open circuit conditions.

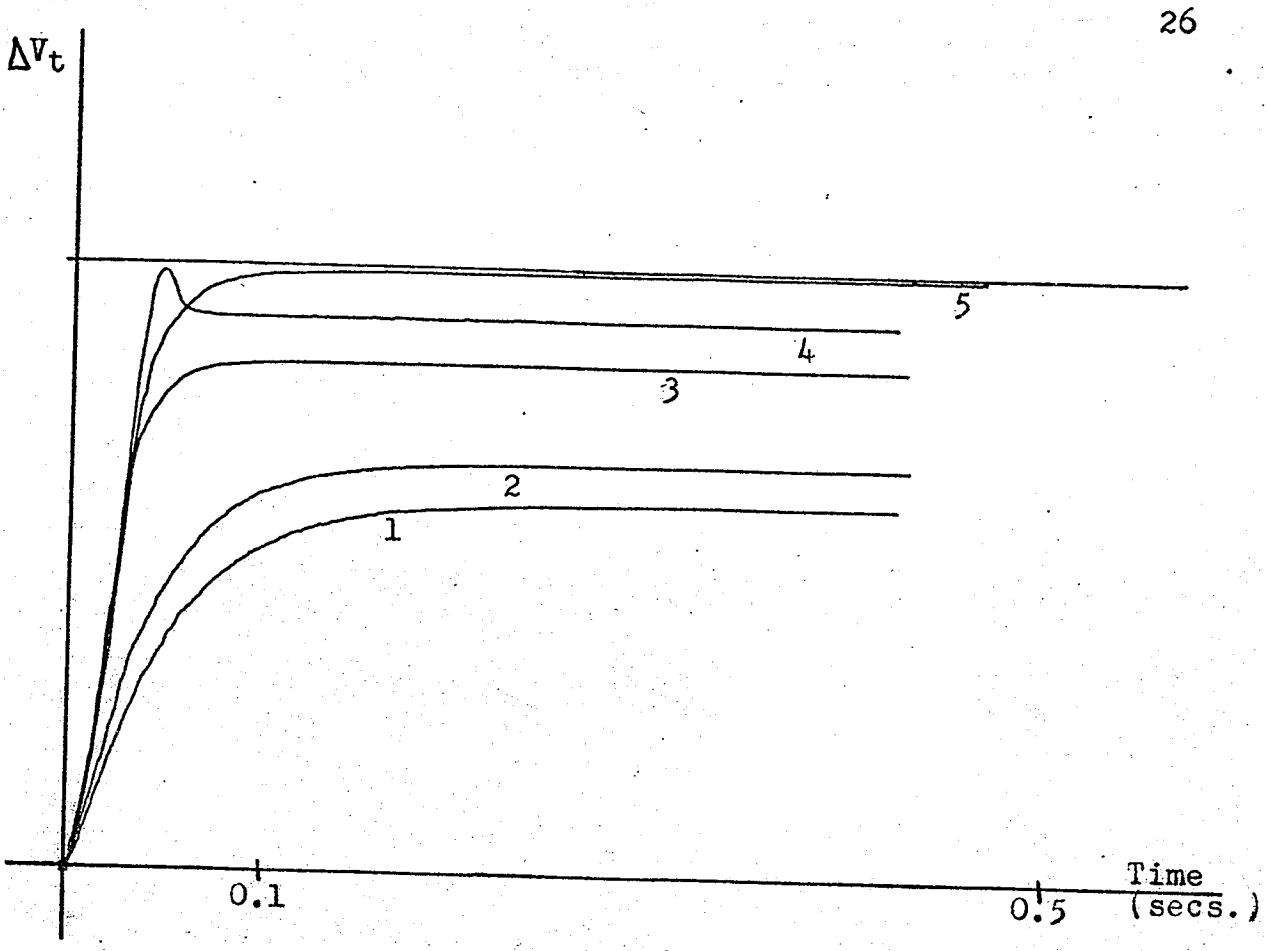

Figure 16. Response of ΔV_t to a Step Command in ΔV_{tRef} Under Open Circuit Conditions for:

1) K_e = 1.5 with no compensation
2) K_e = 2.0 with no compensation
3) K_e = 5.0 with no compensation
4) K_e = 10.0 with no compensation
5) K_e = 5.0 with Lag compensation

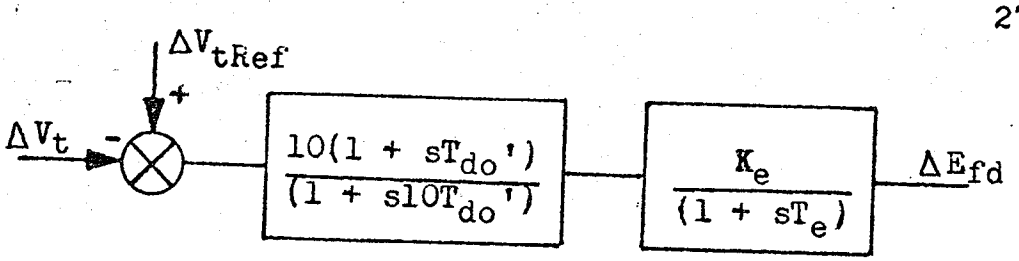

$T_e = 0.005$ secs.

$K_e = 5.0$

$T_{do}' = .120$ secs.

Figure 17. Block Diagram of the Exciter Plus Compensation

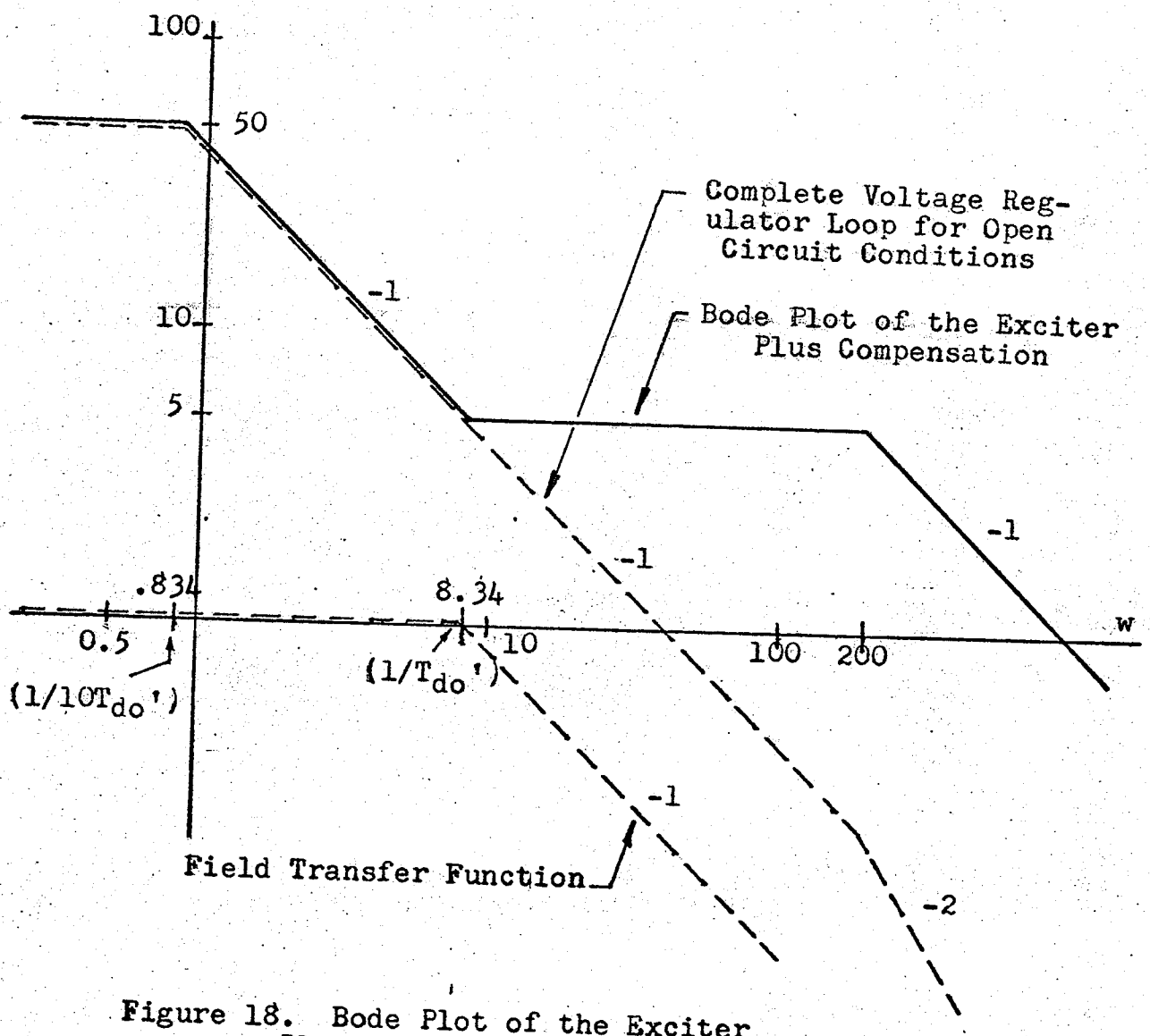

Figure 18. Bode Plot of the Exciter Plus Compensation

IV. REQUIREMENTS OF THE STABILIZING SIGNAL

The concept of synchronizing and damping torques[6] may be applied to establish the basic stabilizing requirements of the system. For constant flux linkage in the direct axis, the system may be represented as in Figure 20 (a). This diagram indicates the two basic stabilizing forces, ΔT_S and ΔT_D, present in the system. All other electrical torques, whether inherent in the machine itself or produced by external stabilizing signals, can be resolved into these two components. The effect of armature reaction is included in Figure 20 (b) by a demagnetizing effect through K_4. At low frequencies the effect is to increase the damping. Under normal transient conditions both the above effects will be present.

Figure 21 includes the voltage regulator in the circuit. The action of the voltage regulator can be divided into two effects: one through K_6, the other through K_5. With the voltage regulator in the circuit, the demagnetizing signal through K_4 now enters the centre of a closed loop formed by K_6 and the exciter. The demagnetizing component is, therefore, reduced by a factor equal to the closed loop gain. The general effect through K_5 is to increase the synchronizing torque for low frequencies but to decrease the synchronizing torque for high frequencies. The damping

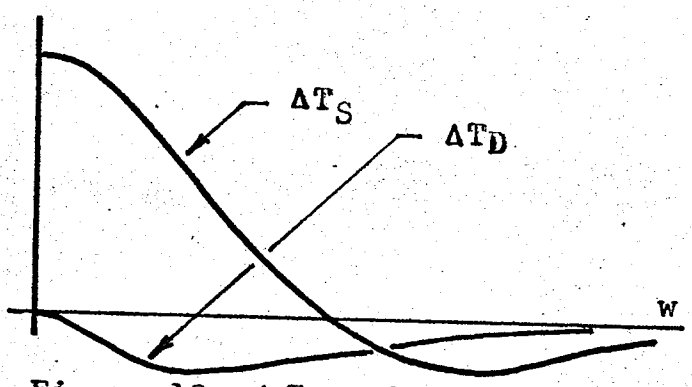

Figure 19. ΔT_S and ΔT_D Produced Through K_5 (For Negative K_5).

torque is reduced for all frequencies. A sketch of synchronizing and damping torques produced through K_5 is shown in Figure 19.

Figure 8 shows the oscillations in the system after a step change in field voltage. These oscillations indicate a lightly damped system with a damping factor of approximately 0.1. The basic stabilizing requirement is, therefore, an increase in system damping both to augment the low natural damping of the system as well as to compensate for the negative damping produced by the voltage regulator. The amount of available synchronizing torque establishes the steady state stability limit of the system. Excessive amounts of synchronizing torque cause higher frequency oscillations and thus reduce the system damping. It also introduces more phase lag into the system and reduces the effectiveness of the stabilizing signals. For the particular system being studied, the synchronizing torque is sufficiently large. In fact, decreasing the synchronizing torque by a small amount often yielded beneficial results. For synchronous machines in general, there is usually an adequately large synchronizing torque component except in cases of extremely high loading or very high external reactance. Under these conditions, it is recommended that the synchronizing torque be increased only enough to produce the desired steady state stability limit. Of course, the damping torque must be increased accordingly.

To increase the system damping a signal proportional to $\Delta\dot{\delta}$ is an obvious choice. With this in mind, the stabilizing loop is shown in Figure 22. The signal is fed through a transfer

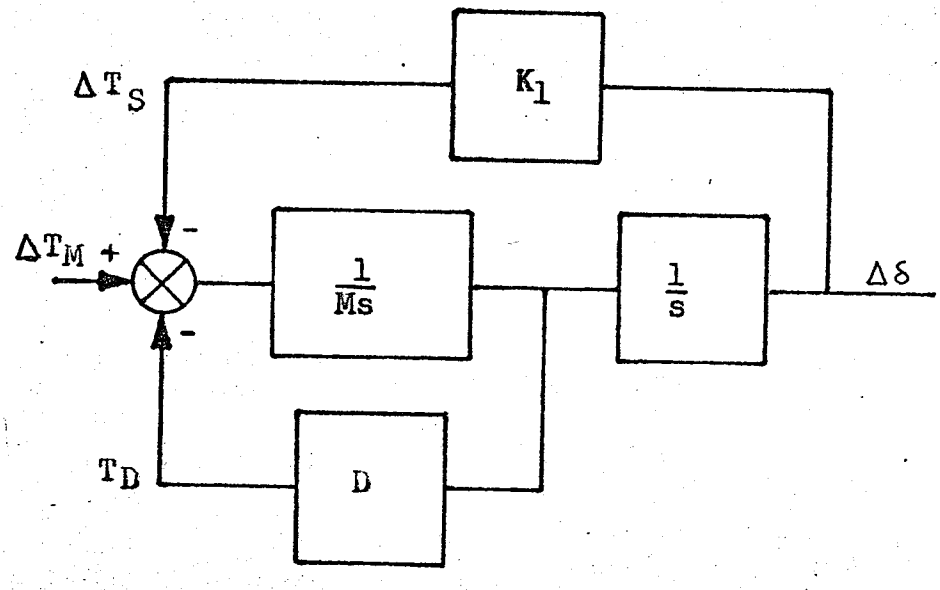

Figure 20a. Second Order Model Showing the Two Basic Stabilizing Forces

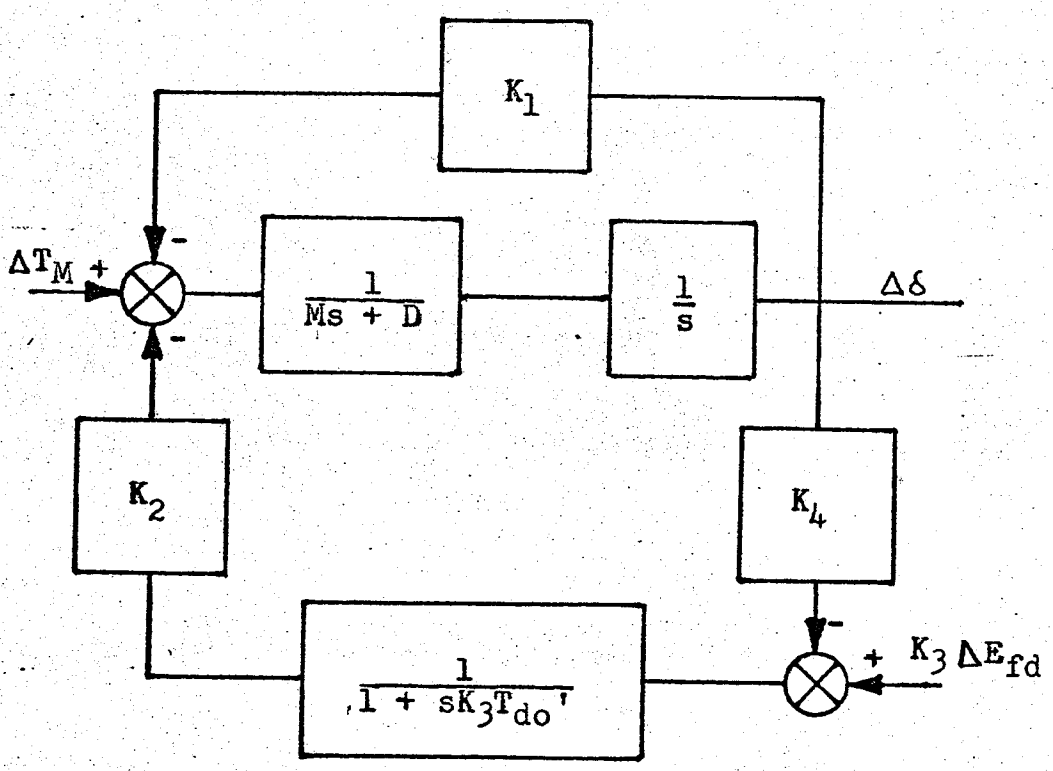

Figure 20b. System Representation Including the Effect of Armature Reaction

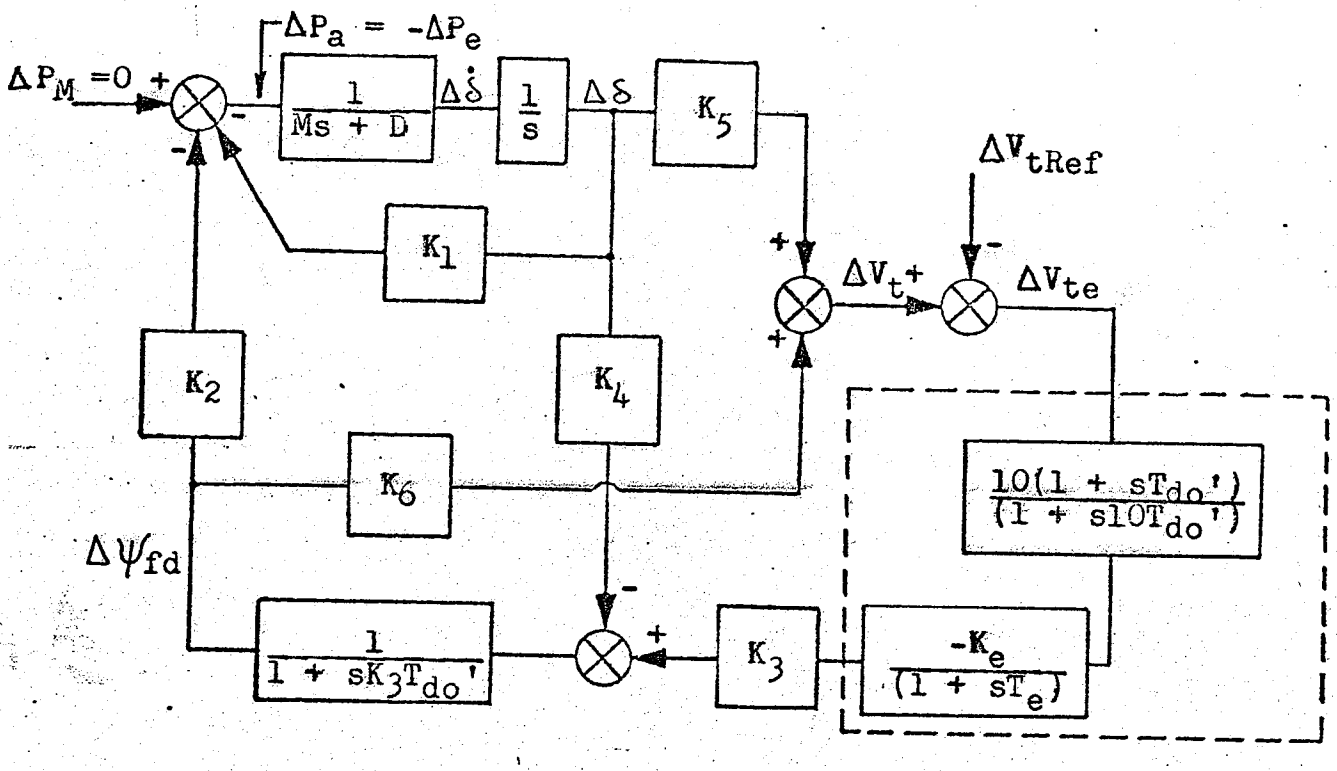

Figure 21. Complete System Representation Including the Voltage Regulator

function G(s) which alters the magnitude and phase of the signal to produce the "best" stabilizing effect. The transfer

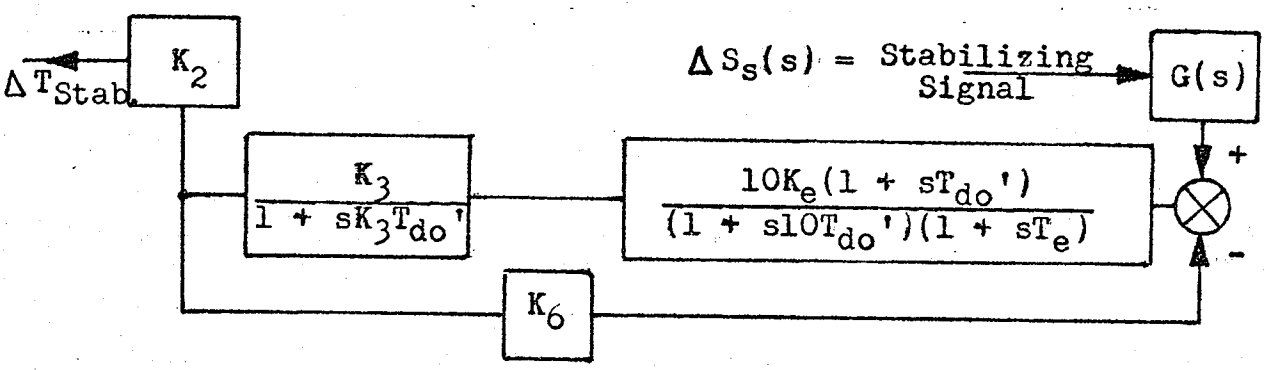

Figure 22. The Stabilizing Loop

function for the stabilization is given in equation (4.1). If the stabilizing signal is proportional to $\Delta\dot{\delta}$ then G(s)

$$\Delta T_{stab.}(s)/\Delta S_s(s) = G(s)\left\{\left[10K_eK_2K_3(1 + sT_{do}')\right] / \left[(1 + s10T_{do}')\,(1 + sT_e)\,(1 + sK_3T_{do}') + 10K_eK_3K_6(1 + sT_{do}')\right]\right\} \qquad (4.1)$$

should provide sufficient phase lead to cancel the phase lag produced in the rest of the transfer function. This would yield pure damping. At a frequency of five hertz, the bracketed term in equation (4.1) contributes approximately seventy degrees of phase lag. Actual values for the magnitude and phase of this term are given in Table 4 for various frequencies of oscillation at the six different operating points.

It is interesting to note that by using a stabilizing signal proportional to accelerating power a phase lead of approximately seventy-eight degrees is added to the stabilizing signal. Exact values for the amount of phase lead introduced by use of a signal proportional to accelerating power are given in Table 5. With G(s) equal to unity and the stabilizing signal proportional to accelerating power the range of

Table 4. Magnitude and Phase of

$$\left[10K_eK_2K_3(1 + sT_{do}')\right] / \left[(1 + s10T_{do}')(1 + sT_e)(1 + sK_3T_{do}') + 10K_3K_6K_e(1 + sT_{do}')\right]$$

Power Factor	x_t(p.u.)	Freq. of Osc. (Hz)	Transfer Function Magnitude	Transfer Function Phase(Deg.) (+ Ind. Lead)
unity	0.0480	3.00	1.13	-52.9
		4.00	0.940	-62.8
		5.00	0.800	-70.3
		6.00	0.690	-76.2
		7.00	0.600	-81.2
0.8 Leading	0.0480	3.00	0.810	-52.8
		4.00	0.680	-62.6
		5.00	0.570	-70.1
		6.00	0.490	-76.1
		7.00	0.430	-81.1
0.8 Lagging	0.0480	3.00	2.11	-53.9
		4.00	1.76	-63.7
		5.00	1.48	-71.1
		6.00	1.27	-77.0
		7.00	1.11	-81.8
unity	0.200	3.00	1.14	-42.6
		4.00	1.00	-52.7
		5.00	0.880	-60.9
		6.00	0.780	-67.7
		7.00	0.690	-73.5
0.8 Leading	0.200	3.00	0.660	-41.7
		4.00	0.580	-51.7
		5.00	0.520	-59.9
		6.00	0.460	-66.8
		7.00	0.410	-72.7
0.8 Lagging	0.200	3.00	1.94	-45.8
		4.00	1.68	-55.9
		5.00	1.45	-64.0
		6.00	1.27	-70.6
		7.00	1.12	-76.1

Table 5. Phase Lead Produced by Use of a Stabilizing Signal Proportional to Accelerating Power

Freq. of Osc. (Hz.)	Phase Lead (Deg.)
3.00	69.9
4.00	74.6
5.00	77.6
6.00	79.6
7.00	81.1

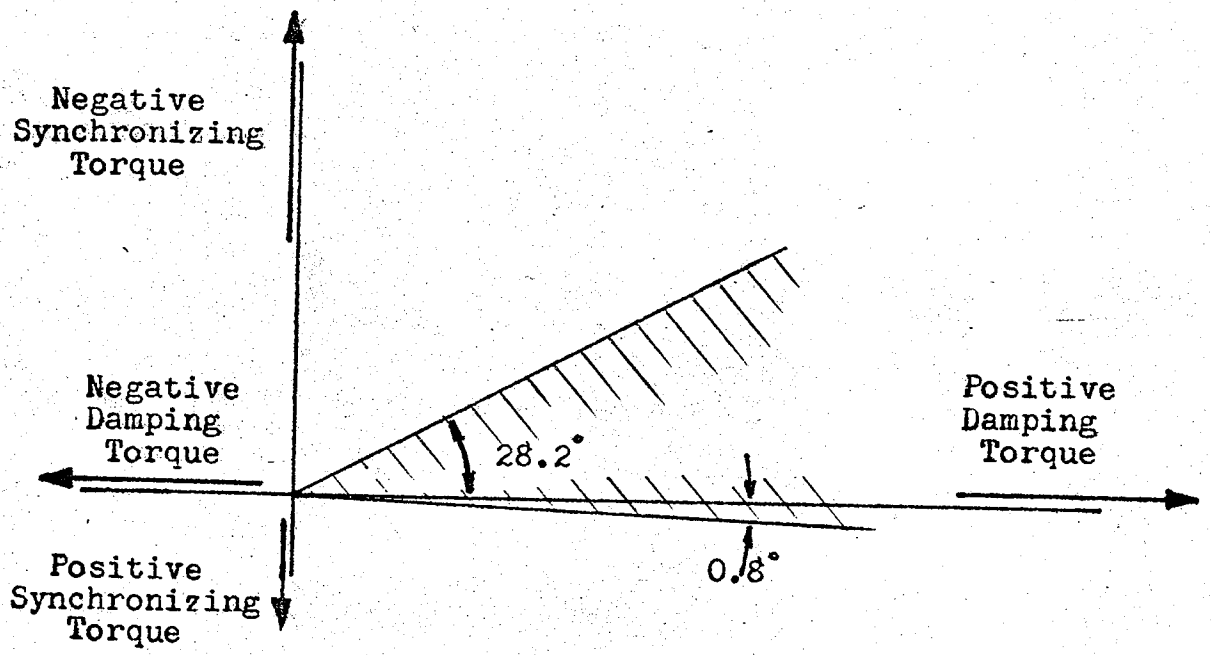

Figure 23. Sector Showing the Range of Values For the Phase of the Complete Transfer Function of the Stabilizing Loop with G(s) Equal to Unity and the Stabilizing Signal Proportional to Accelerating Power

values for the phase of the complete transfer function given in equation (4.1) is shown in Figure 23. It is apparent that for all six operating conditions and for a considerable range of frequency about the normal five hertz value, a stabilizing signal proportional to accelerating power provides the necessary damping component without seriously affecting the synchronizing torque. The sector shown in Figure 23 could be reduced in size or shifted in either direction by the use of additional compensation. For this particular study, however, this is not considered necessary and no additional compensation is considered.

V. ANALOG COMPUTER TESTS AND RESULTS

Analog computer tests were performed to evaluate and compare the effects of bang-bang and proportional stabilization. Figure 24 shows the complete analog computer simulation of the system including voltage regulation and stabilizing signals. For convenience, the simulation has been slowed down by a factor of ten. All test results, however, are given on a real time basis. For easy comparison of results, the disturbance in each case was made equal to a one per unit step change in mechanical torque input. Unless otherwise indicated, all tests were performed with the machine delivering rated power at unity power factor and with an external reactance of 0.0480 per unit.

Comparison of Figures 25 and 26 indicates the effect of the voltage regulator. The most noticeable difference is the smaller steady state change in field voltage with the voltage regulator in the circuit. A closer inspection of the two figures indicates that the damping is slightly reduced in Figure 26. This effect was predicted earlier in Chapter 5.

Figures 26 - 31 illustrate the effects of proportional and equivalent bang-bang stabilizing signals related to accelerating power. The basis of equivalence between these signals is their maximum amplitude. In all tests this amplitude was adjusted to a value of three per unit. In the case of bang-bang stabilization, the stabilizing signal always has a value of plus or minus three per unit but with proportional stabilization,

only the first swing of the stabilizing signal reaches a value of three per unit. These results indicate that a bang-bang stabilizing signal damps out oscillations in accelerating power much faster than an equivalent proportional signal. Bang-bang stabilization does, however, introduce low frequency oscillations in the torque angle. These oscillations are entirely internal to the system and do not affect the terminal behaviour of the machine. Therefore, as long as these torque angle oscillations eventually die away, they are not considered to be as important as the oscillations in accelerating power or terminal voltage. Terminal voltage was not included in the figures because the oscillations were of very low amplitude. Measurements indicated that the deviation in terminal voltage was never more than 0.05 per unit.

Figure 32 shows the effect of a bang-bang stabilizing signal in phase with $\Delta\dot{\delta}$. This signal increases both components of torque with emphasis on the synchronizing component yet stability is not maintained. This illustrates the fact that excessive amounts of synchronizing torque are detrimental to system stability.

The effect of the stabilizing signal amplitude is shown in Figure 33. The bang-bang nature of the field voltage appears to be superimposed on a lower frequency under damped oscillation and it becomes apparent that voltage regulating action contributes a significant portion of the field voltage variations especially for high values of stabilizing signal amplitude. For example, a bang-bang stabilizing signal of five per unit produces variations as large as nine per unit in field voltage. This effect was also present in Figure 30 where a three per unit bang-bang signal was used.

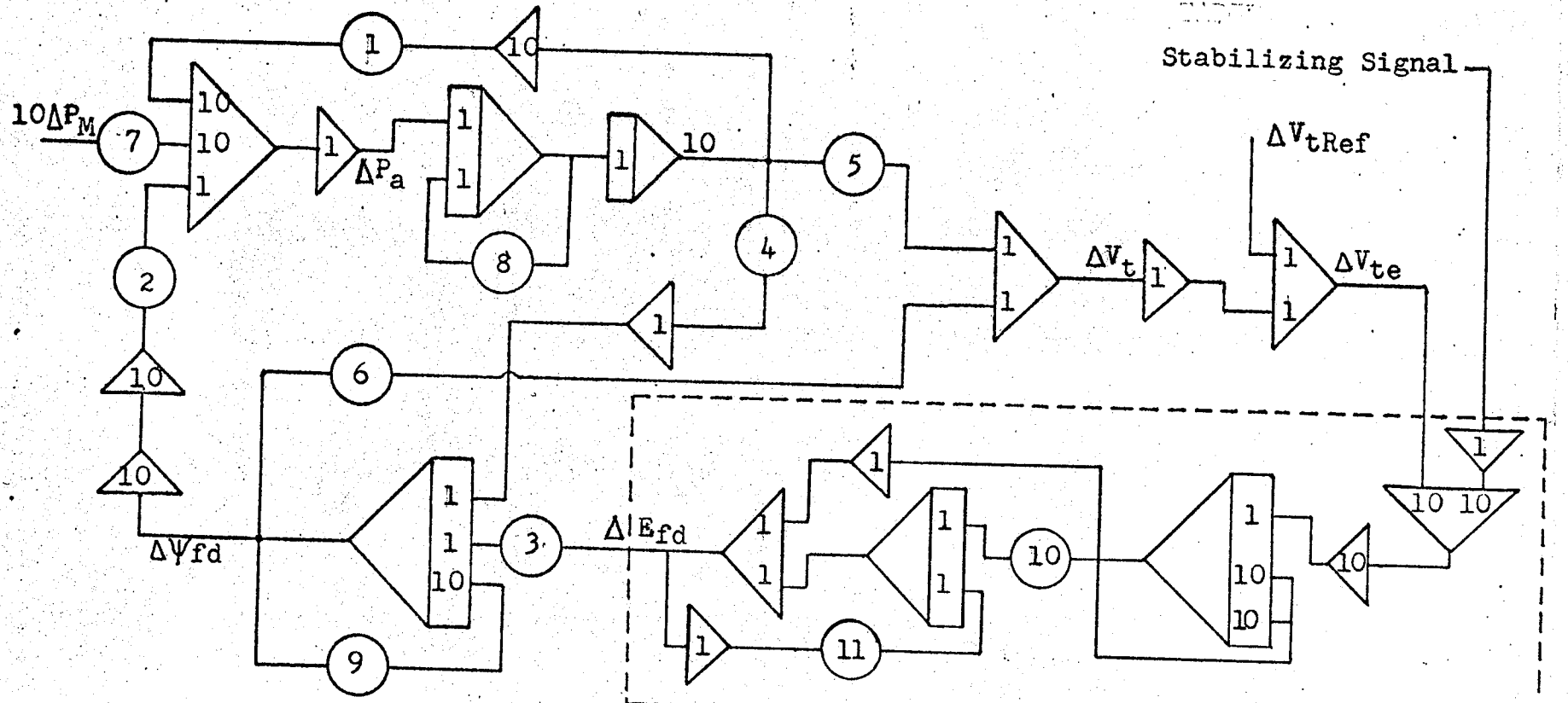

Pot Settings Given By:

#1 = .0605 K_1	#4 = .127 K_4	#7 = .605	#10 = .834
#2 = .605 K_2	#5 = - .1 K_5	#8 = .690	#11 = .0834
#3 = 1.27 K_3	#6 = K_6	#9 = .127	

Figure 24. Complete Analog Computer Simulation of the System Including Time Scaling

In that case the field voltage reached a maximum value of four per unit. Returning to Figure 33, it is apparent that when a one per unit stabilizing signal is used the effect of the voltage regulator on field voltage is almost negligible. As bang-bang stabilizing signal amplitudes become higher, the fraction of field voltage deviation caused by voltage regulator action increases. Eventually a point is reached where bang-bang stabilization cannot be considered as effective as conventional proportional control. Experiments indicate that this point occurs beyond a ten per unit level of field voltage. Therefore, if one assumes that exciter ceiling voltages do not exceed ten per unit, then bang-bang stabilization will always produce "better" results than proportional stabilization producing equal maximum deviation in field voltage.

Another problem innerent in the use of a bang-bang control signal is the fact that the signal cannot remain indefinitely. Once the disturbance has been sufficiently damped, the stabilization must be removed. Several alternatives are available, the easiest of which is a simple switching operation. The signal may be switched off after all transients have died away yielding results identical to those given in Figures 30 and 31. No additional transient is produced. The signal may also be removed before the transients have completely died away. This is illustrated in Figure 34.

Figure 35 illustrates the universal nature of the stabilization. Without modifying the signal in any way, increased damping is achieved at all six operating points. Four of the resulting trajectories are shown in Figure 35.

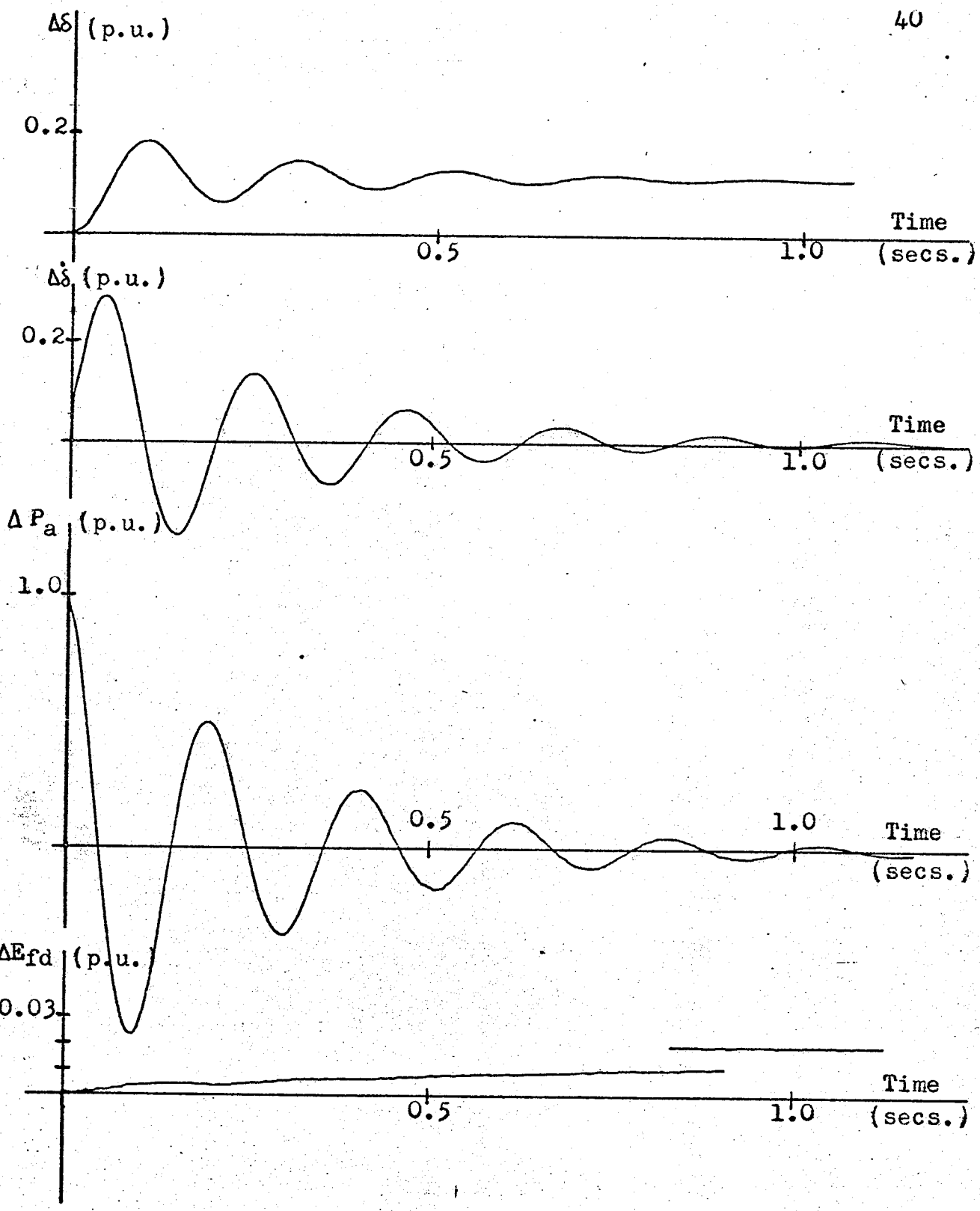

Figure 25. Dynamic Stability With No Voltage Regulator and No Stabilizing Signal

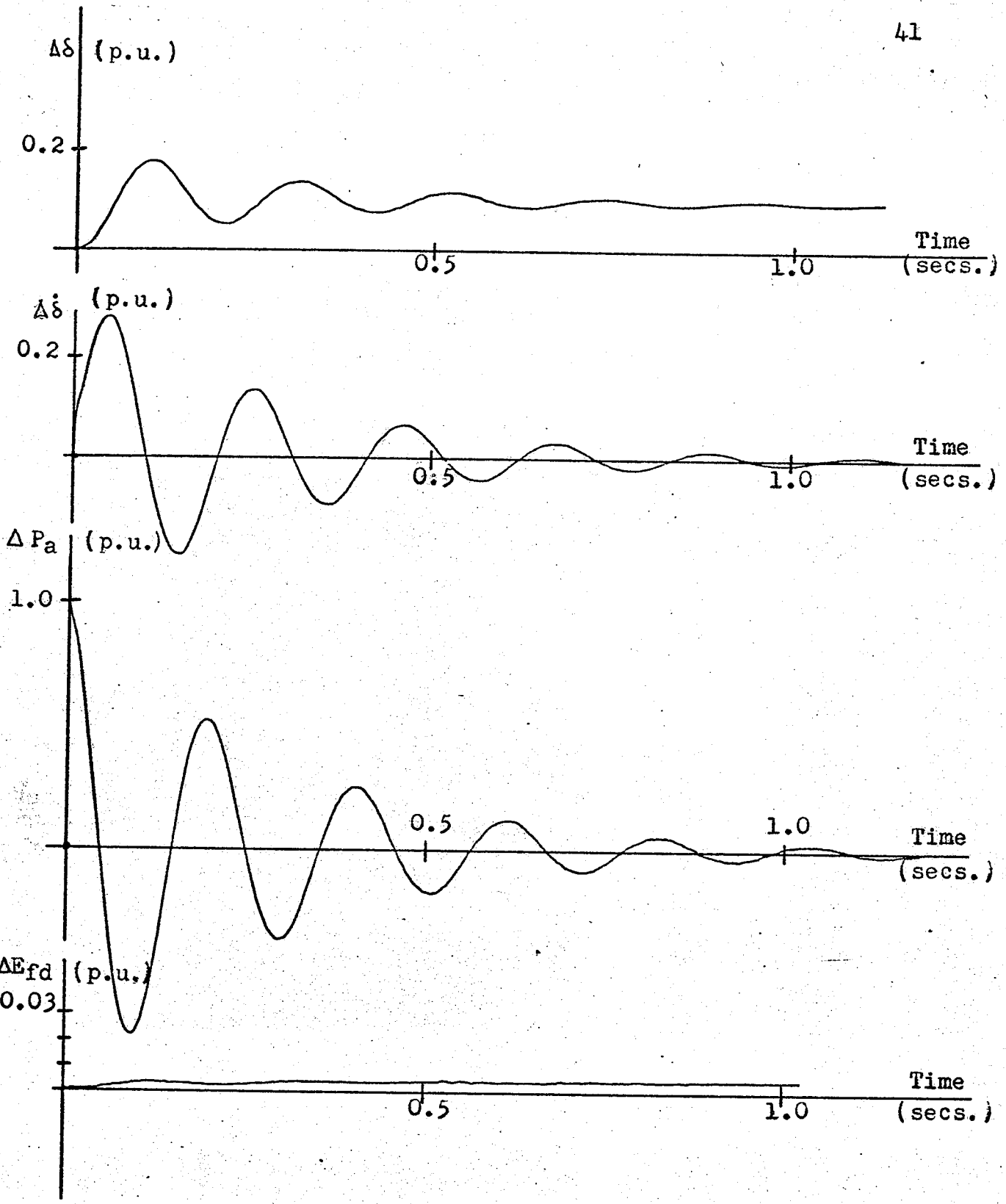

Figure 26. Dynamic Stability With Voltage Regulator But No Stabilizing Signal

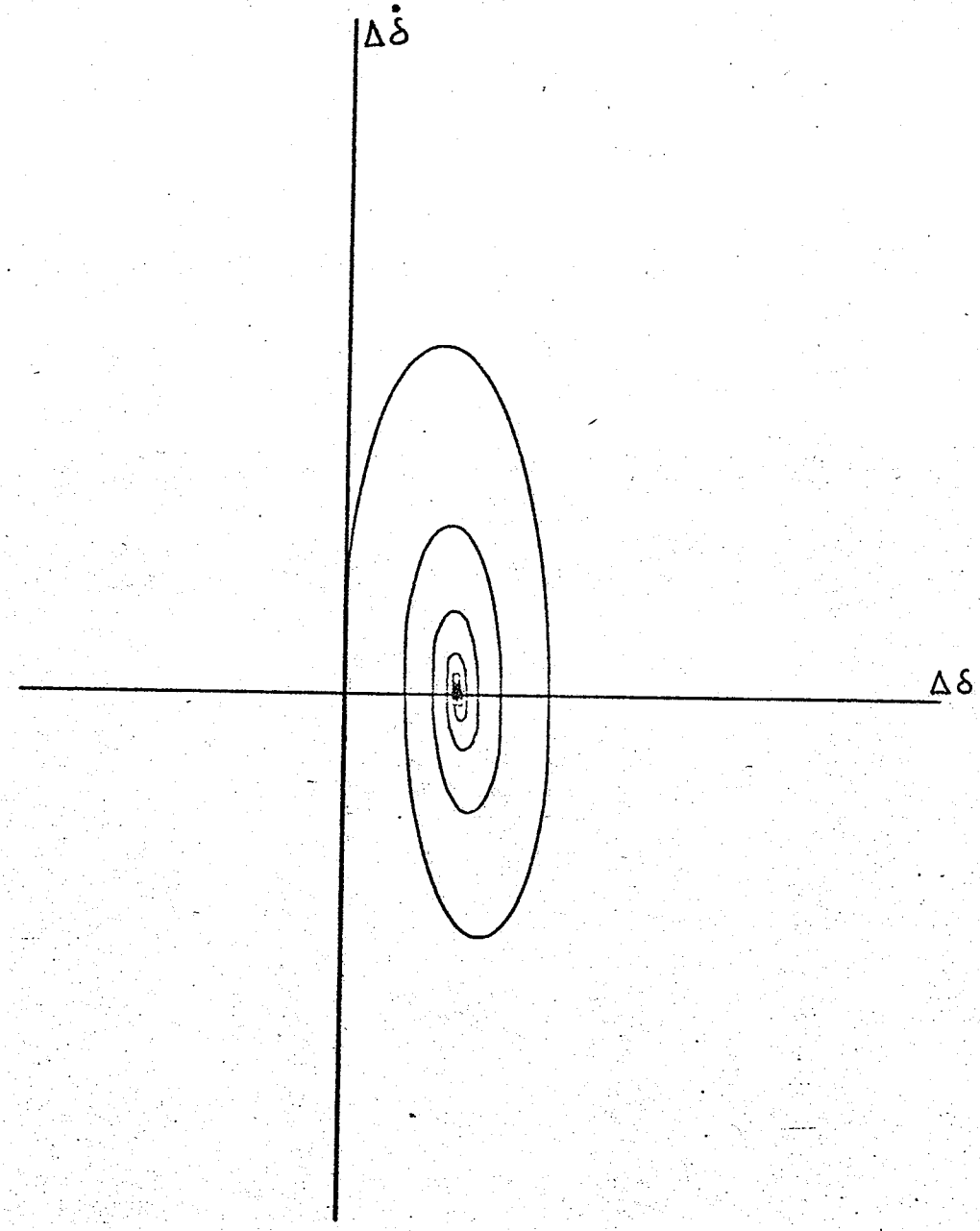

Figure 27. $\Delta\dot{\delta}$ Versus $\Delta\delta$ With Voltage Regulator But No Stabilizing Signal

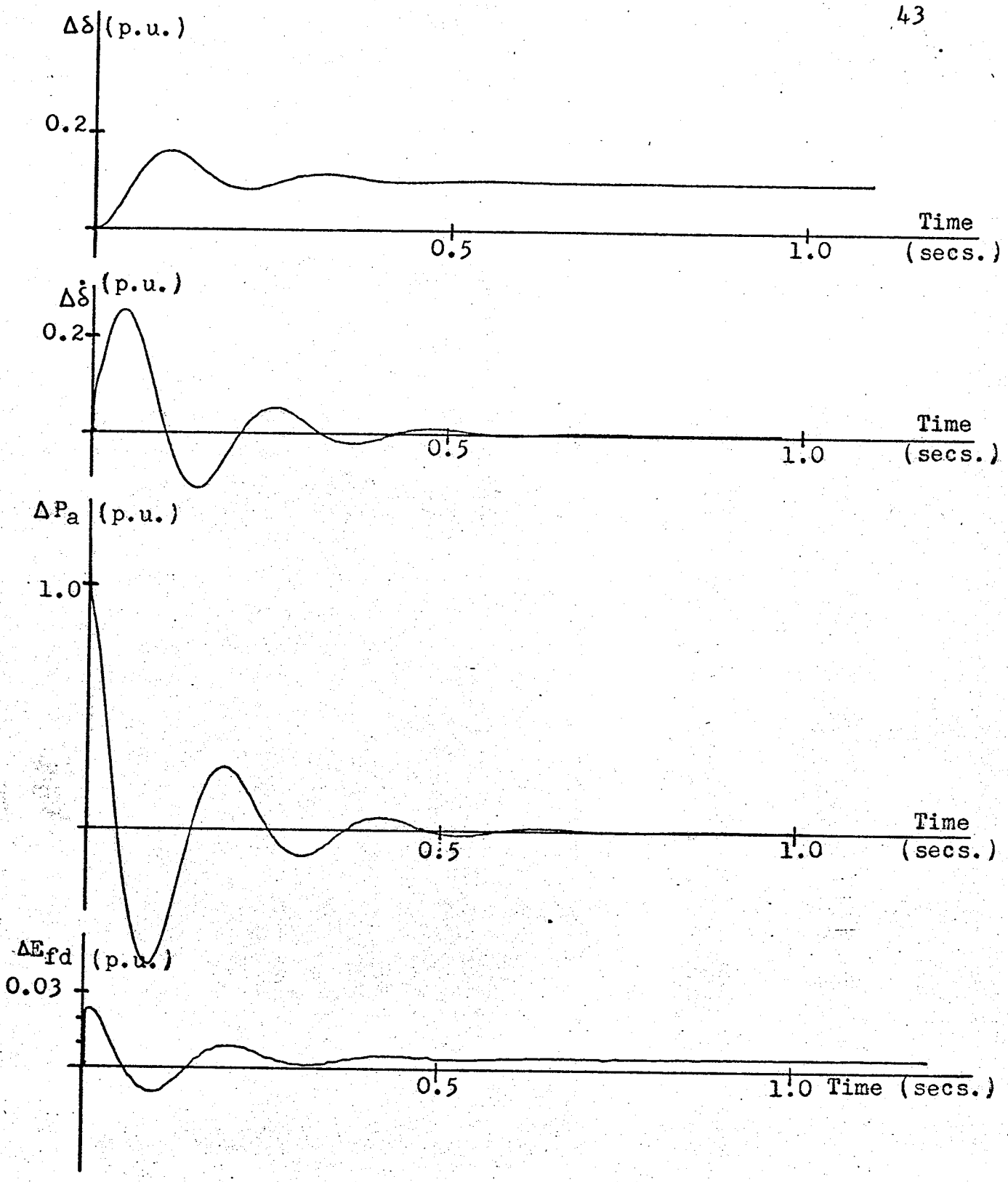

Figure 28. Dynamic Stability With Stabilizing Signal Proportion to ΔP_a

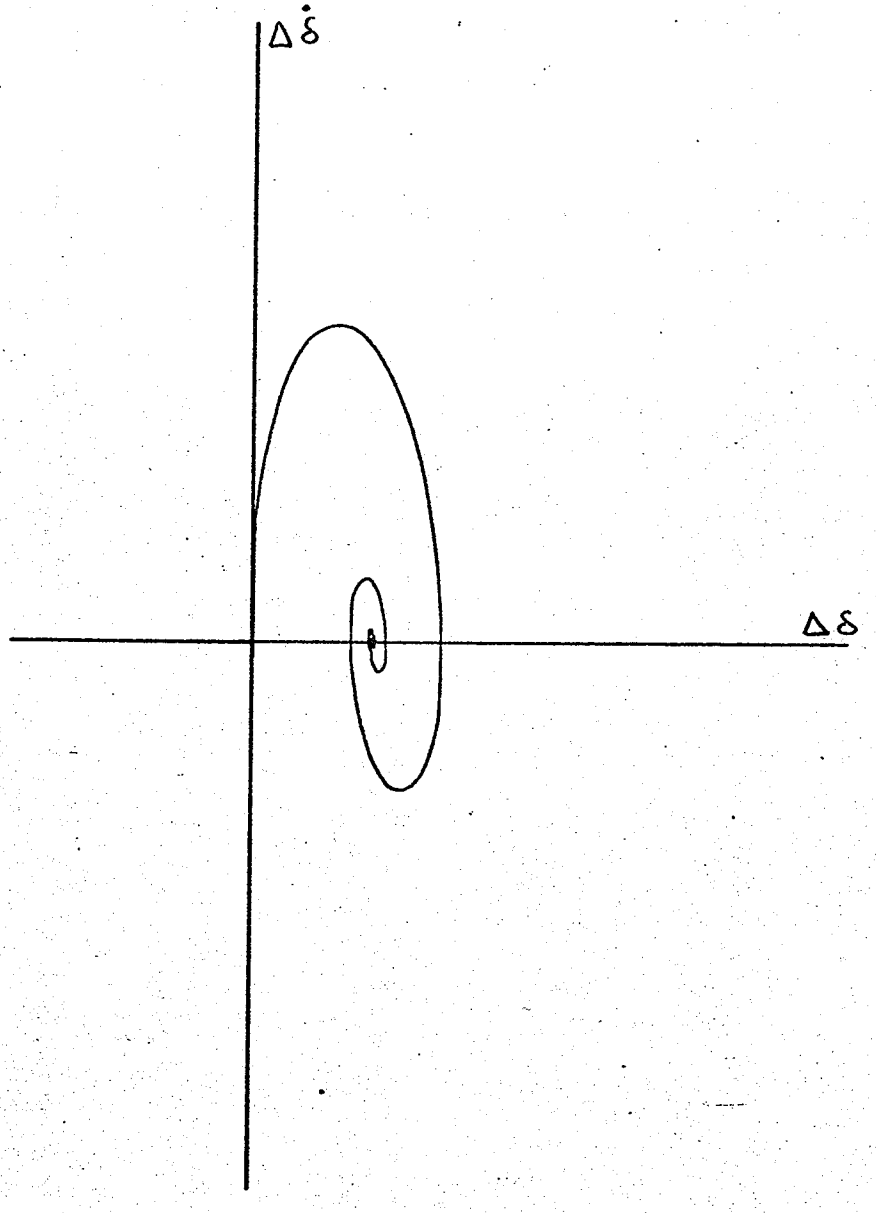

Figure 29. $\Delta\dot{\delta}$ Versus $\Delta\delta$ With Proportional Stabilizing Signal

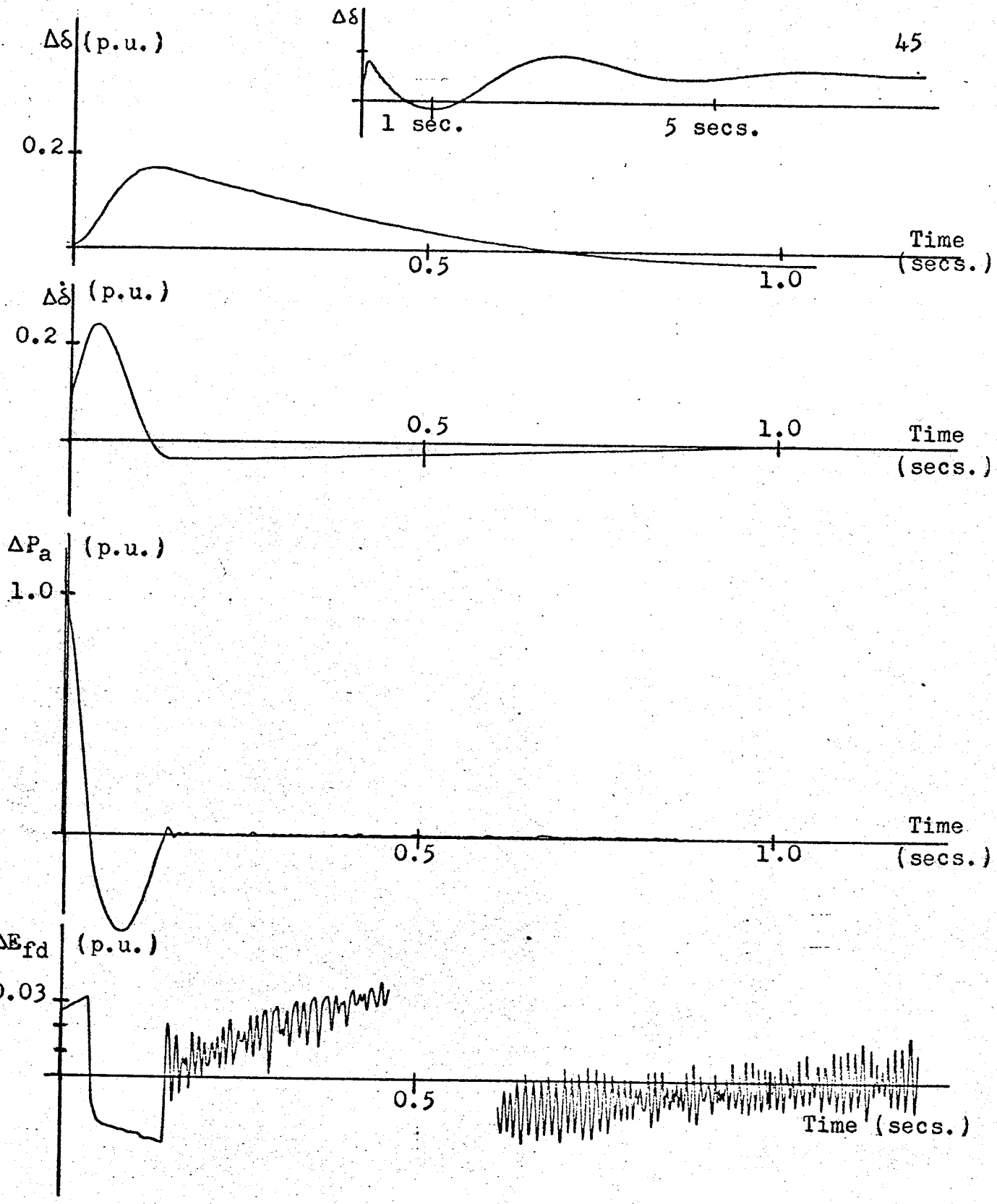

Figure 30. Dynamic Stability With Bang-Bang Stabilizing Signal in Phase With ΔP_a

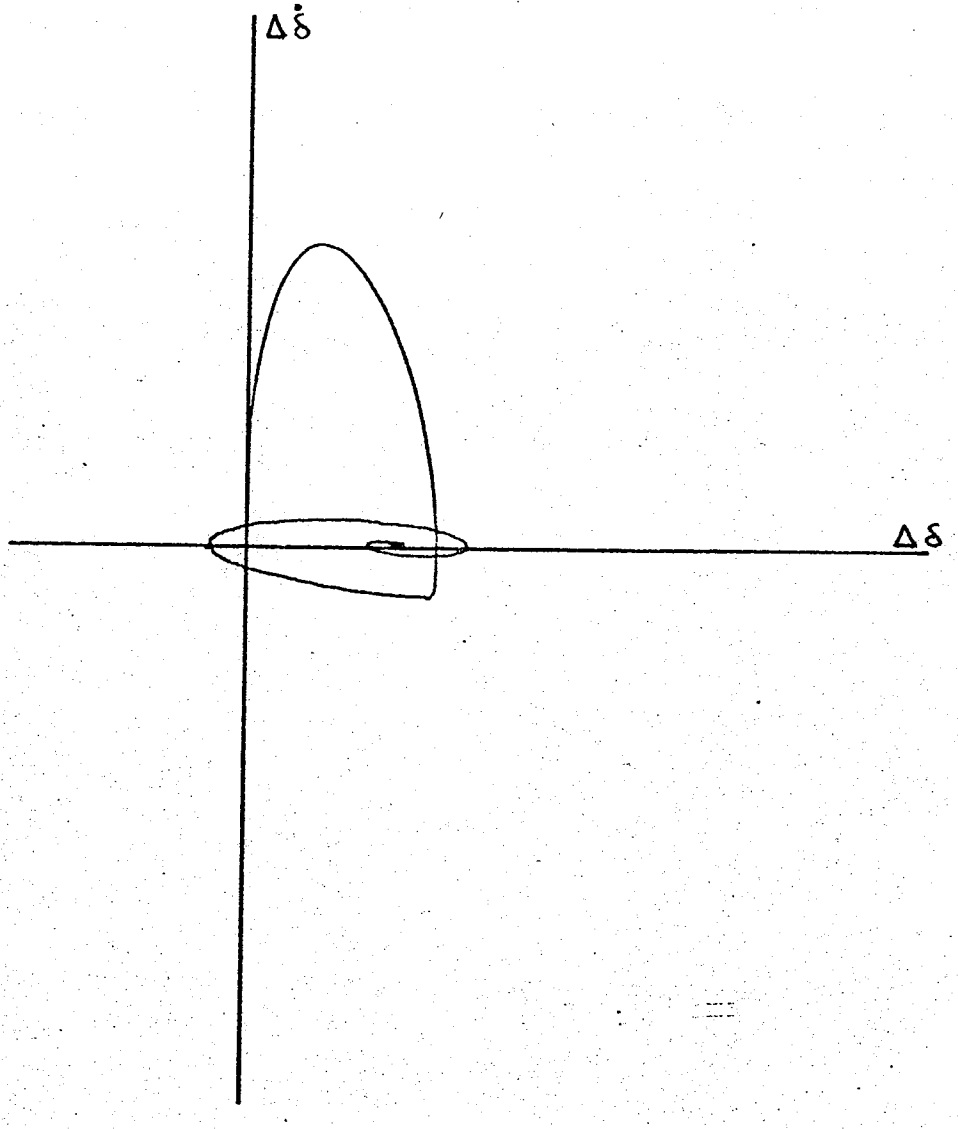

Figure 31. $\Delta\dot{\delta}$ Versus $\Delta\delta$ With Bang-Bang Stabilizing Signal

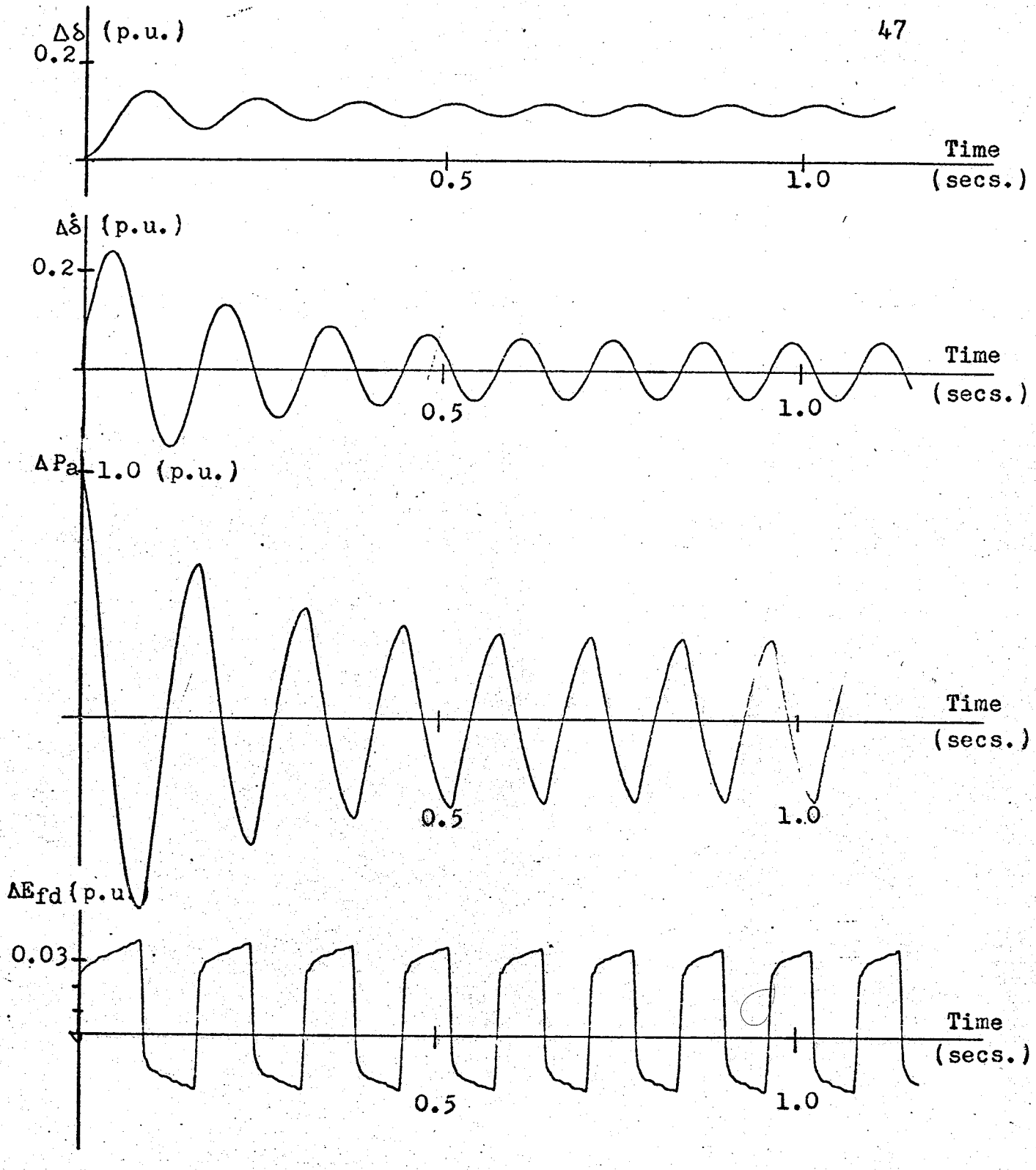

Figure 32. Dynamic Stability With Bang-Bang Stabilizing Signal in Phase With $\Delta\dot{\delta}$

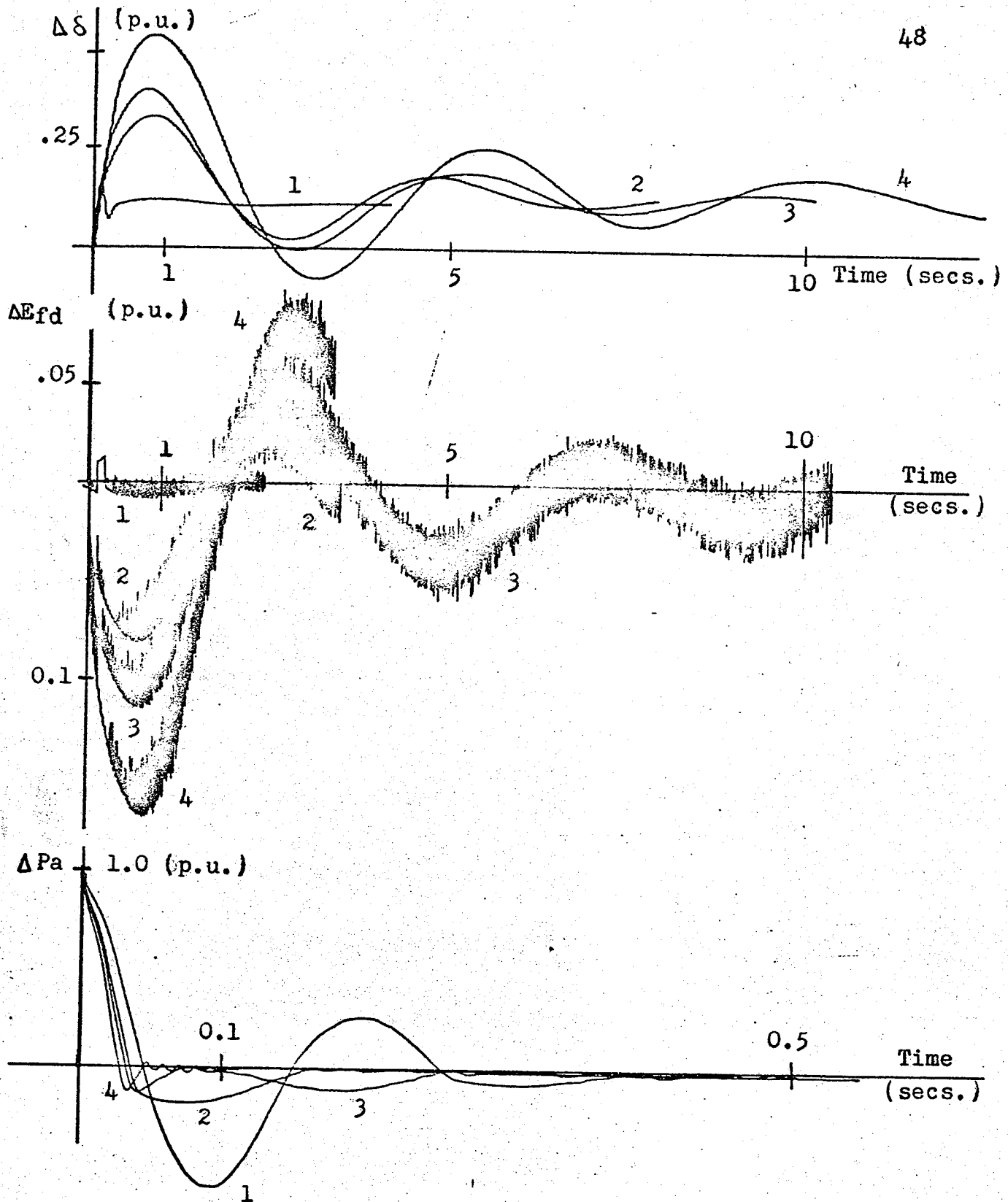

Figure 33. Dynamic Stability with Bang-Bang Stabilization and Stabilizing Signal Ceiling Voltages of:

1) 1 p.u. 2) 5 p.u. 3) 7 p.u. 4) 10 p.u.

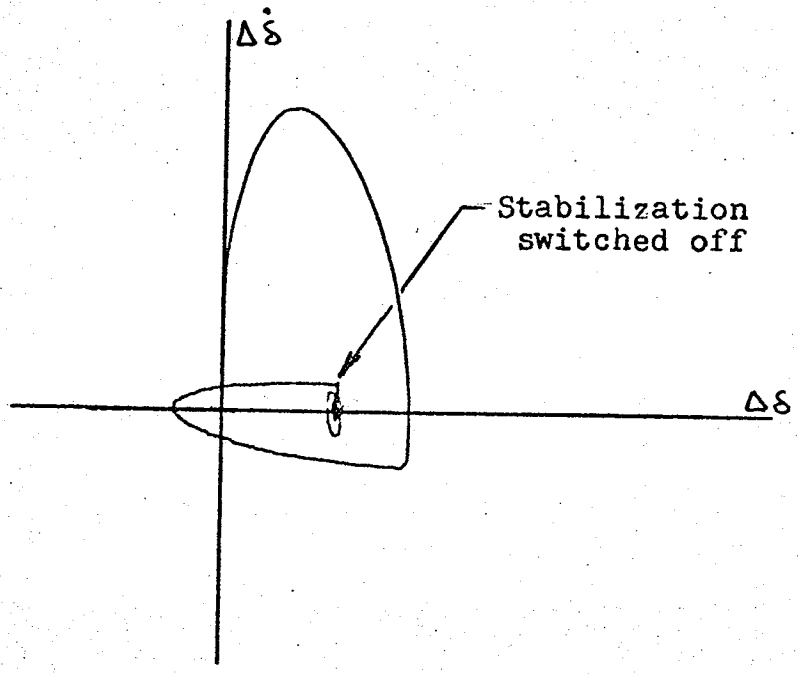

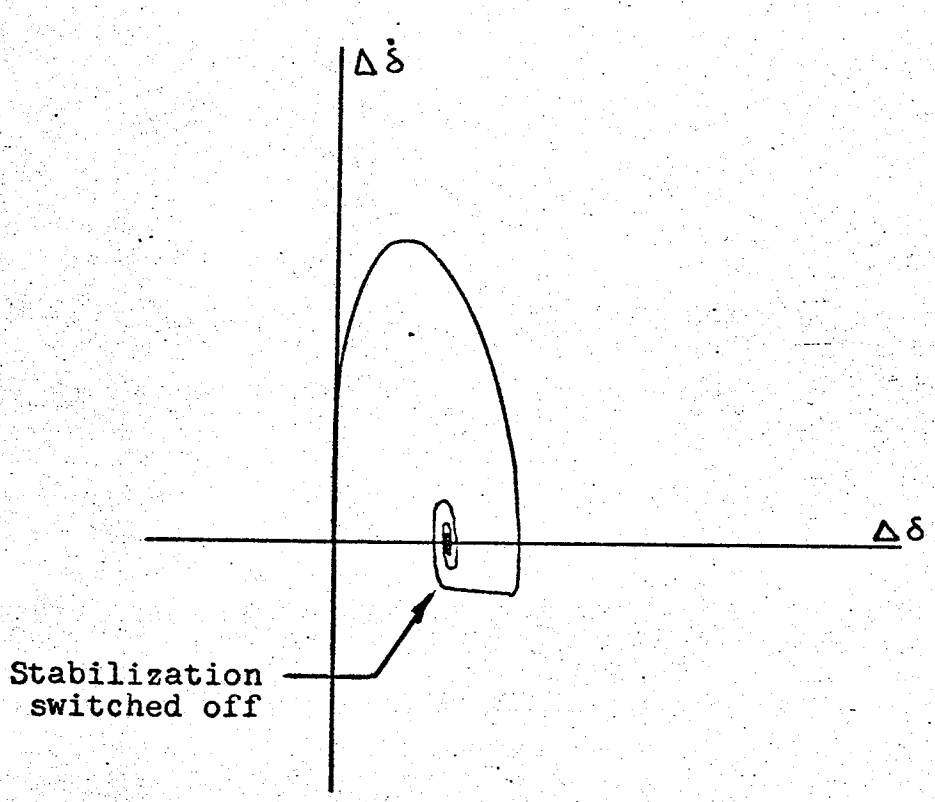

Figure 34. Showing the Effect of Switching Off the Bang-Bang Signal

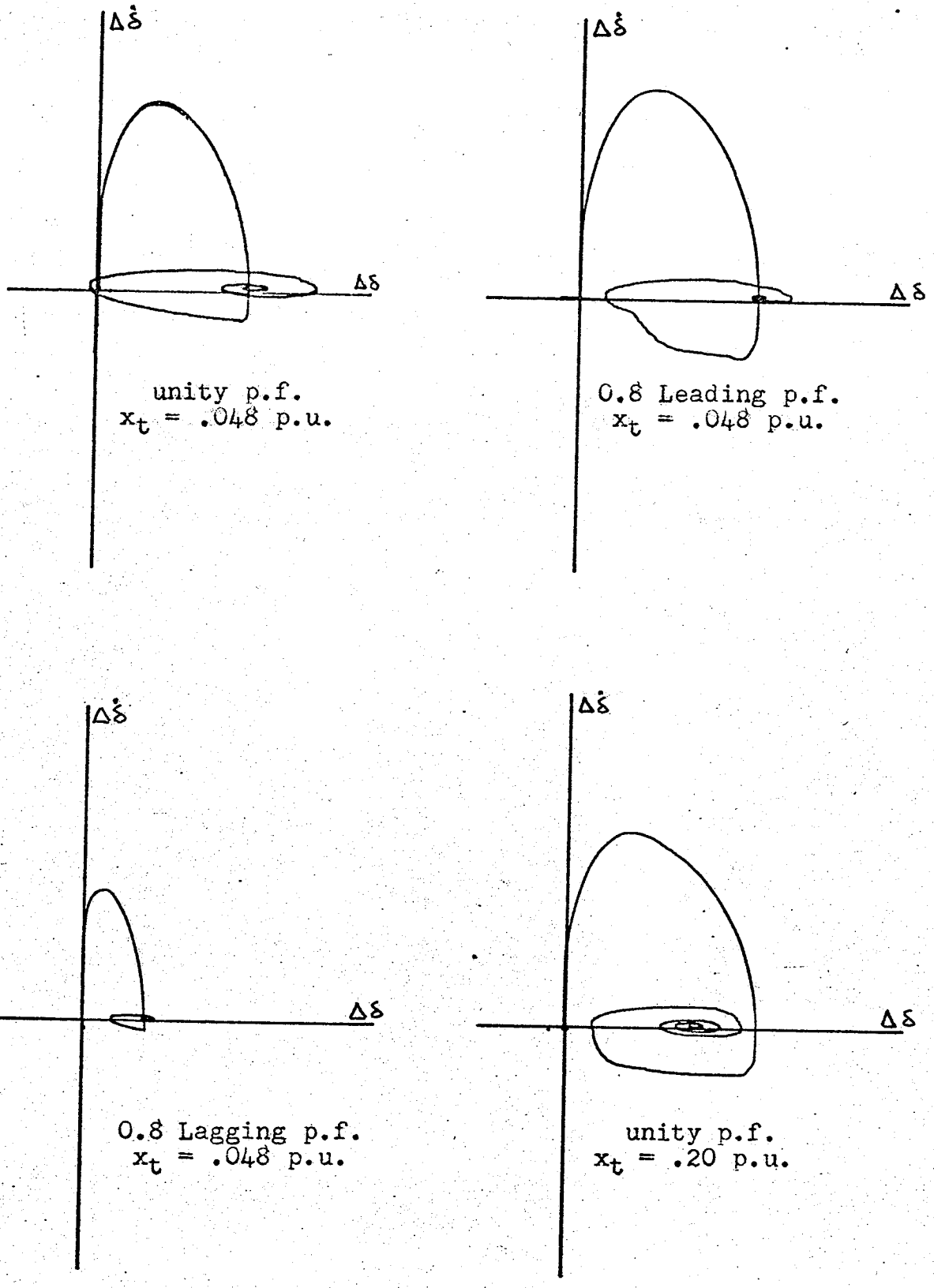

Figure 35. $\Delta\dot{\delta}$ Versus $\Delta\delta$ for Four Different Operating Points

VI. GENERAL CONCLUSIONS

The results of the analog computer tests indicate that a stabilizing signal proportional to accelerating power can produce significant improvements in the system's dynamic stability. It has also been shown that an equivalent bang-bang signal related to accelerating power provides even greater improvements in the damping of the system. Furthermore, as indicated in Appendix A, the bang-bang stabilization is easily applied to actual machines. The stabilization was also found to be effective at several different operating points. This is due to the fact that the signal becomes an integral part of the system providing a feedback path similar to those producing the natural damping and synchronizing torque compenents. The compensation does not rely on previously determined information or switching times. It has been indicated that for even more diversified operating conditions, additional phase correction may be used to increase the effectiveness of the signal. This implies that this form of stabilization would be useful in the more general case of a machine in a power system where many modes of oscillation between machines and groups of machines may occur.

A. TECHNIQUE FOR OBTAINING ELECTRICAL POWER AND ACCELERATING POWER SIGNALS

Under three-phase balanced conditions the total electrical power is a constant (i.e. a d.c. value). If voltage and current of each phase are multiplied together to yield three power signals, and these signals are in turn added, the resulting control signal will be a d.c. voltage indicating the electrical power output of the machine. Accelerating power is obtained by subtracting the above signal from a signal proportional to the mechanical input power. In this study governor action was neglected and mechanical power was assumed constant and equal to the steady state electrical power. The block diagram of Figure 36 illustrates the method used to obtain control signals proportional to electrical and accelerating powers. Since losses are neglected, the mechanical input power must equal the electrical output power under steady state conditions. If governor action is to be included, the mechanical power signal during transient conditions may be derived from the pre-fault electrical power output signal[24].

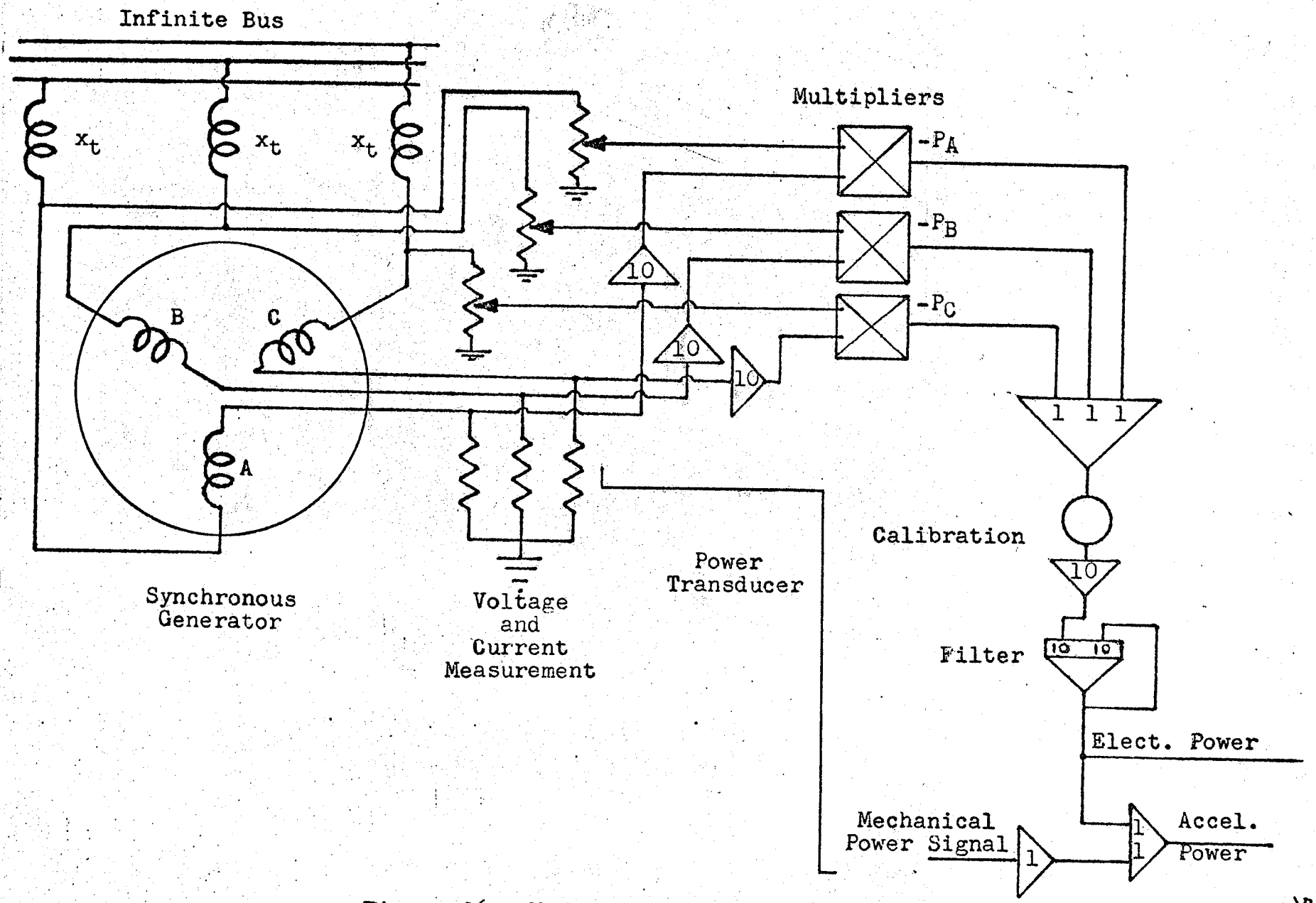

Figure 36. Measurement of Electrical Power and Accelerating Power

B. LIST OF SYMBOLS

D	Per unit damping constant
E_{fd}	Field voltage of the machine
I_d	Projection of stator current on the direct axis
I_q	Projection of stator current on the quadrature axis
I_{fd}	Field current of the machine
K_e	Exciter gain
M	Per unit inertia constant (equals $H/\pi f$)
P_a	System accelerating power
P_e	Electrical output power
P_M	Mechanical input power
s	Laplace transform variable
T_a	System accelerating torque
T_d'	Machine short circuit time constant
T_{do}'	Machine open circuit time constant
T_D	Natural damping torque of the machine
T_e	Electrical torque
T_M	Mechanical input torque
T_S	Natural synchronizing torque of the machine
V_b	Infinite bus voltage
V_d	Projection of the bus voltage on the direct axis
V_q	Projection of the bus voltage on the quadrature axis
V_t	Machine terminal voltage
V_{tdo}	Projection of machine terminal voltage on the direct axis
V_{tqo}	Projection of the machine terminal voltage on the quadrature axis
V_{tRef}	Terminal voltage reference

V_{to}	Machine terminal voltage error (equals $(V_t - V_{tRef})$)
x_d	Direct axis synchronous reactance
x_d'	Direct axis transient reactance
x_q	Quadrature axis synchronous reactance
x_t	External reactance (simulating a transmission line)
ψ_d	Direct axis flux linkages
ψ_{fd}	Field flux linkages
ϕ	Power factor angle in degrees
δ	Torque angle (angle between quadrature axis and infinite bus voltage)

The zero subscript indicates that the quantity is evaluated at an operating point.

Δ indicates a small excursion about the initial operating point.

Dots above the symbol indicate differentiation with respect to time.

BIBLIOGRAPHY

1. Athans, M. and P. L. Falb. Optimal Control (book), McGraw-Hill Book Co., 1966.

2. Blythe, A. L., "The Effect of Static Excitation Characteristics on System Stability," presented to the Canadian Electrical Association (Planning and Operations Section), March 1967.

3. Coles, H. E., "Dynamic Performance of a Turbo-Alternator Utilizing 3-Term Governor Control and Voltage Regulation," IEEE Proceedings, Vol. 115, #2, Feb. 1968, pp. 266-279.

4. Concordia, C., "Effect of Buck-Boost Voltage Regulator on Steady State Power Limit," Trans. AIEE (Part 1), Vol. 69, 1950, pp. 380-385.

5. Dandeno, Paul, L., and others, "Effect of High-Speed Rectifier Excitation Systems on Generator Stability Limits," IEEE Trans. on Power Apparatus and Systems, Vol. Pas-87, No. 1, Jan. 1968, pp. 190-201.

6. Demello, Francisco P., "Concepts of Synchronous Machine Stability as Effected by Excitation Control," IEEE Trans. on Power Apparatus and Systems, Vol. Pas-88, No. 4, April 1969, pp. 316-329.

7. Dineley, J. L., A. J. Morris, and C. Preece, "Optimized Transient Stability From Excitation Control of Synchronous Generators," IEEE Trans. on Power Apparatus and Systems, Vol. Pas-87, No. 8, Aug. 1968, pp. 1696-1705.

8. Dorf, Richard C., Modern Control Systems (book), Addison-Wesley Pub. Co., 1967

9. Fitzgerald, A. E., and Kingsley, Charles, Electric Machinery (book), McGraw-Hill Book Co., 1961.

10. Heffron, W. G. and R. A. Phillips, "Effect of a Modern Amplidyne Voltage Regulator on Under-excited Operation of Large Turbine Generators," Trans. AIEE (Power Apparatus and Systems), Vol. 71, Aug. 1952, pp. 692-697.

11. Jones, G. A., "Transient Stability of a Synchronous Generator Under Conditions of Bang-Bang Excitation Scheduling," IEEE Trans. on Power Apparatus and Systems, Vol. Pas-84, Feb. 1965, pp. 114-121.

12. Kimbark, E. W., Power System Stability (book), Vol. III, John Wiley and Sons, 1948-1956.

13. Laughton, M. A., "Matrix Analysis of Dynamic Stability in Synchronous Multimachine Systems," IEEE Proceedings, Vol. 113, No. 2, Feb. 1966, pp. 325-336.

14. Laws, Frank, A., Electrical Measurements (book), McGraw-Hill Book Company, Inc., 1938.

15. Mittelstadt, William, A., "Four Methods of Power System Damping," IEEE Trans. on Power Apparatus and Systems, Vol. Pas-87, No. 5, May 1968, pp. 1323-1329.

16. Nath, N. G. and A. K. Choudhury, "Posicast and Negicast Control Systems," Int. J. Control, Vol. 9, No. 5, May 1969, pp. 509-533

17. Park, R. H., "Two-Reaction Theory of Synchronous Machines: I-Generalized Method of Analysis," Trans. AIEE, Vol. 48, July 1929, pp. 716-730.

18. Rankin, A. W., "The Equations of the Idealized Synchronous Machine," General Electric Review, Vol. 47, June 1944, pp. 31-36

19. Sarma, V. V. S., and others, "Effect of Intermittent Regulation on Power System Steady State Stability," Int. J. Control, 1967, Vol. 6, No. 3, pp. 241-248.

20. Schleif, Ferber R., and others, "Excitation Control to Improve Powerline Stability," IEEE Trans. on Power Apparatus and Systems, Vol. Pas-87, No. 6, June 1968, pp. 1426-1434.

21. Smith, O. J. M., "Posicast Control of Damped Oscillatory Systems," IRE Proceedings, Vol. 45, Sept. 1957, pp. 1249-1255.

22. Smith, O. J. M., "Optimal Transient Removal in a Power System," IEEE Trans. on Power Apparatus and Systems, Vol. Pas-84, No. 5, May 1965, pp. 361-374.

23. Stevenson, William, D., Jr., Elements of Power System Analysis (book), 2nd Ed., McGraw-Hill Book Co., 1962

24. Sud, S., "Stabilization of Paralleled Static-and-Amplidyne-Excited Synchronous Machines," M.Sc. Thesis, University of Manitoba, 1969.

25. Swift, G. W., "A Laboratory Experiment on Transient Stability," IEEE Trans. on Education, Vol. E-11, No. 2, June 1968, p. 156.

26. Wright, Sherwin, H., "Determination of Synchronous Machine Constants by Test," Trans. AIEE, Vol. 50, Dec. 1931, pp. 1331-1351.

27. Yu, Yao-nan, Khien Vongsuriya, and Leonard Wedman, "Application of an Optimal Control Theory to a Power System," Paper No. 69 TP-104-PWR. Presented at Winter Power Conf., New York, Jan. 1969.